# Antiproton constraints on Dark Matter

Gaëlle Giesen

Institut de Physique Théorique (IPhT) - CEA Saclay

WIN '13 Sept 19th

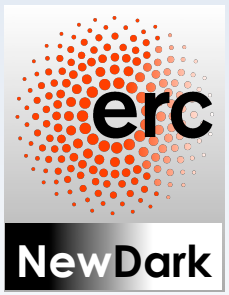


DM annihilation or decay in the halo of our Galaxy
$\Rightarrow$ Cosmic Ray propagation (convection, diffusion, etc...)
$\Rightarrow$ Detection at Earth

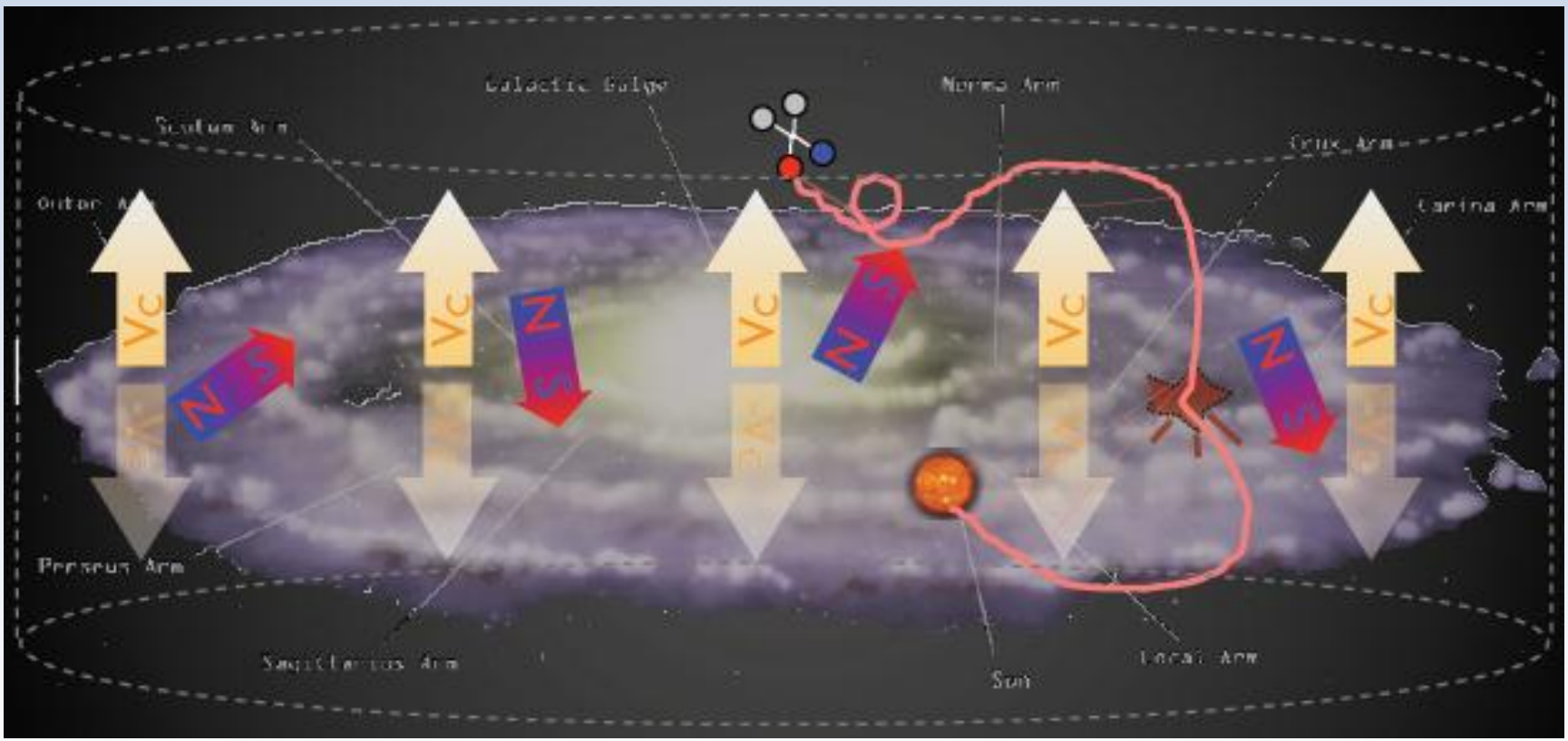

Indirect Dark Matter search : (DM) $\mathrm{DM} \rightarrow \mathrm{prim}\ \mathrm{prim} \rightarrow ... \rightarrow \bar{p}$

Indirect Dark Matter search : $(\mathrm{DM})\ \mathrm{DM} \rightarrow \mathrm{prim}\ \mathrm{prim} \rightarrow ... \rightarrow \bar{p}$

- For annihilation (decay) into quark or gauge bosons
  $\Rightarrow$ hadronization produces antiprotons

Indirect Dark Matter search : (DM) $\mathrm{DM} \to \mathrm{prim}\ \mathrm{prim} \to \ldots \to \bar{p}$

- For annihilation (decay) into quark or gauge bosons
  $\Rightarrow$ hadronization produces antiprotons
- For annihilation (decay) into leptons
  $\Rightarrow$ electroweak corrections give antiprotons

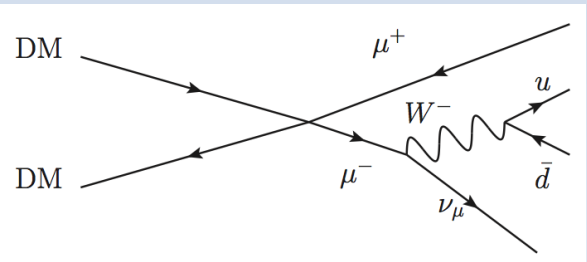

Indirect Dark Matter search : (DM) $\mathrm{DM} \rightarrow \mathrm{prim}\ \mathrm{prim} \rightarrow ... \rightarrow \bar{p}$

- For annihilation (decay) into quark or gauge bosons
  $\Rightarrow$ hadronization produces antiprotons
- For annihilation (decay) into leptons
  $\Rightarrow$ electroweak corrections give antiprotons

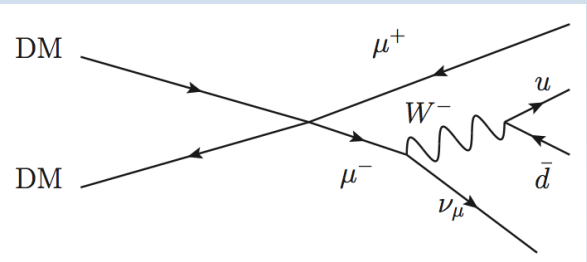


- Astrophysical background : small uncertainties in the $\mathrm{GeV} - \mathrm{TeV}$ range $\Rightarrow$ detection of a WIMP signal

Indirect Dark Matter search : (DM) $\mathrm{DM} \to \mathrm{prim}\ \mathrm{prim} \to ... \to \bar{p}$

- For annihilation (decay) into quark or gauge bosons
  $\Rightarrow$ hadronization produces antiprotons
- For annihilation (decay) into leptons
  $\Rightarrow$ electroweak corrections give antiprotons

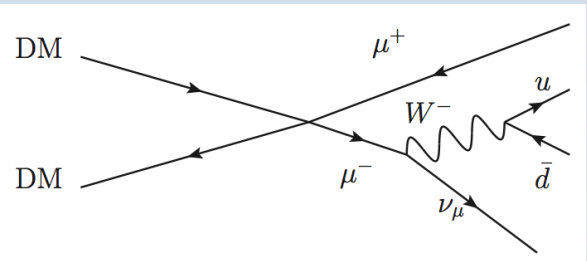


- Astrophysical background : small uncertainties in the $\mathrm{GeV} - \mathrm{TeV}$ range $\Rightarrow$ detection of a WIMP signal
- Current PAMELA data already very competitive

Indirect Dark Matter search : (DM) $\mathrm{DM} \to \mathrm{prim}\ \mathrm{prim} \to ... \to \bar{p}$

- For annihilation (decay) into quark or gauge bosons
  $\Rightarrow$ hadronization produces antiprotons
- For annihilation (decay) into leptons
  $\Rightarrow$ electroweak corrections give antiprotons

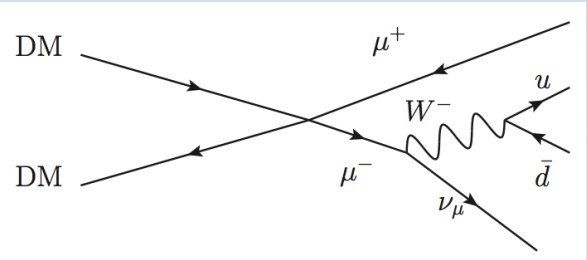


- Astrophysical background : small uncertainties in the $\mathrm{GeV} - \mathrm{TeV}$ range $\Rightarrow$ detection of a WIMP signal
- Current PAMELA data already very competitive
- Upcoming AMS-02 data even more precise
  $\Rightarrow$ Forecast : sensitivities and reconstruction capabilities

- DM Annihilation/decay channels

$$\left.\begin{array}{rr} \text{annihilation} & \text{DM DM} \\ \text{decay} & \text{DM} \end{array}\right\} \rightarrow b\bar{b}, t\bar{t}, W^+W^-, ZZ, \mu^+\mu^-, \tau^+\tau^-, \gamma\gamma$$

- DM Annihilation/decay channels

$$\left.\begin{array}{rl} \text{annihilation} & \text{DM DM} \\ \text{decay} & \text{DM} \end{array}\right\} \rightarrow b\bar{b}, t\bar{t}, W^+W^-, ZZ, \mu^+\mu^-, \tau^+\tau^-, \gamma\gamma$$

- DM halo profiles

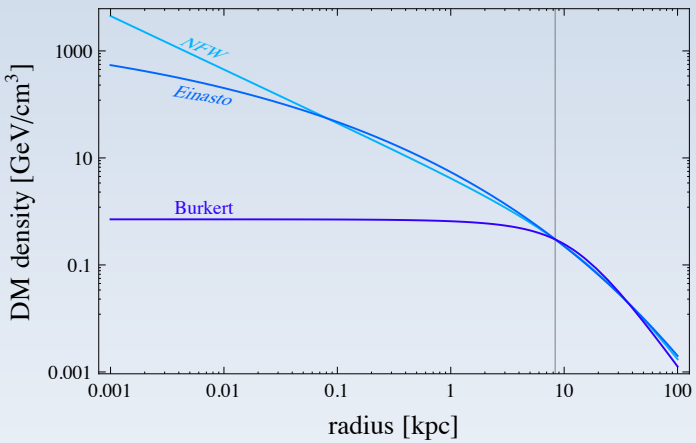

- DM Annihilation/decay channels

$$\left.\begin{array}{rl} \text{annihilation} & \text{DM DM} \\ \text{decay} & \text{DM} \end{array}\right\} \rightarrow b\bar{b}, t\bar{t}, W^+W^-, ZZ, \mu^+\mu^-, \tau^+\tau^-, \gamma\gamma$$

- DM halo profiles

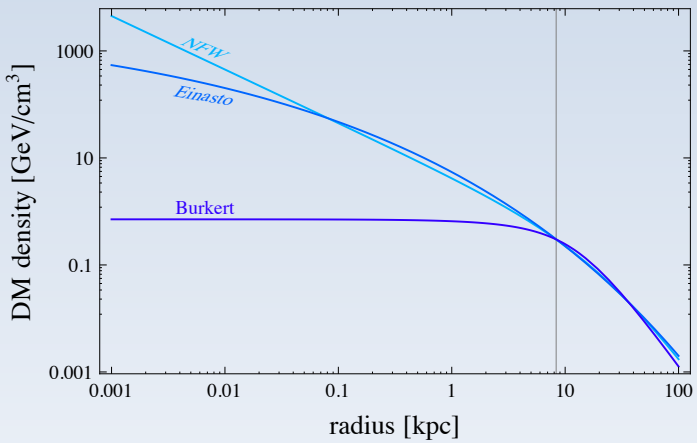


- Antiproton propagation in the galactic halo

| Model | $\delta$ | $\mathcal{K}_0$ [kpc$^2$/Myr] | $V_{\rm conv}$ [km/s] | $L$ [kpc] |
|---|---|---|---|---|
| MIN | 0.85 | 0.0016 | 13.5 | 1 |
| MED | 0.70 | 0.0112 | 12 | 4 |
| MAX | 0.46 | 0.0765 | 5 | 15 |

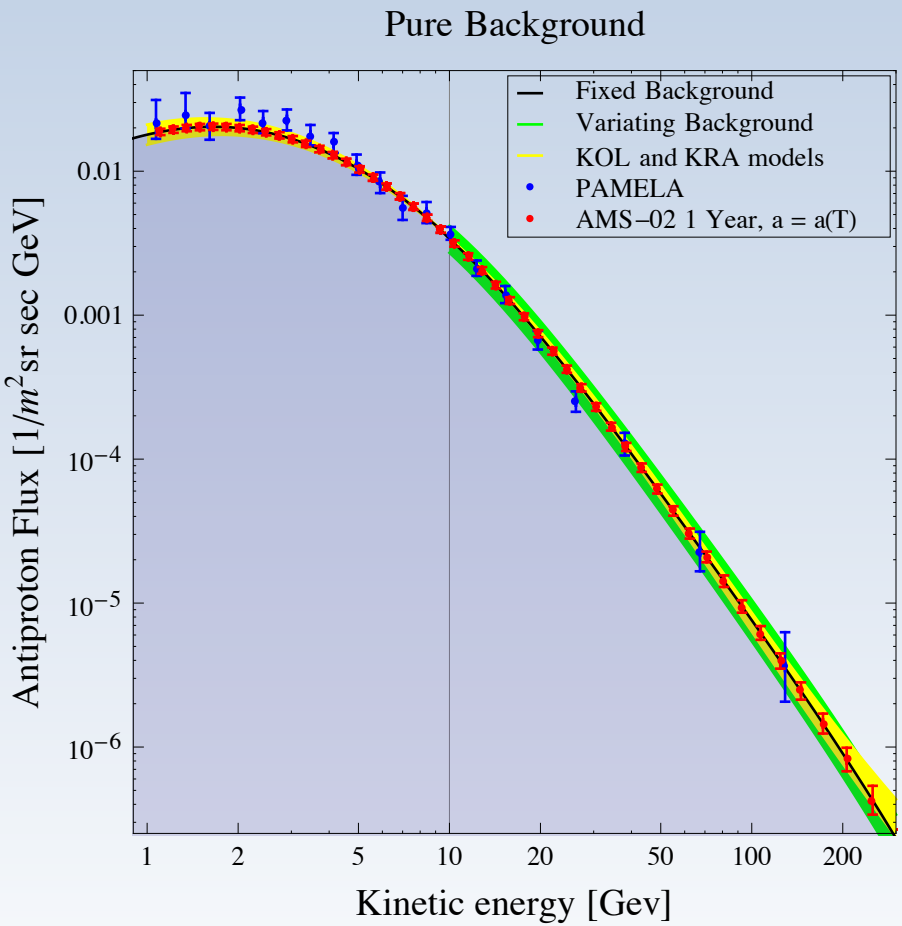


- Fixed Background
  $\phi_{\text{fixed}}(T > 10\,\text{GeV})$ : power law

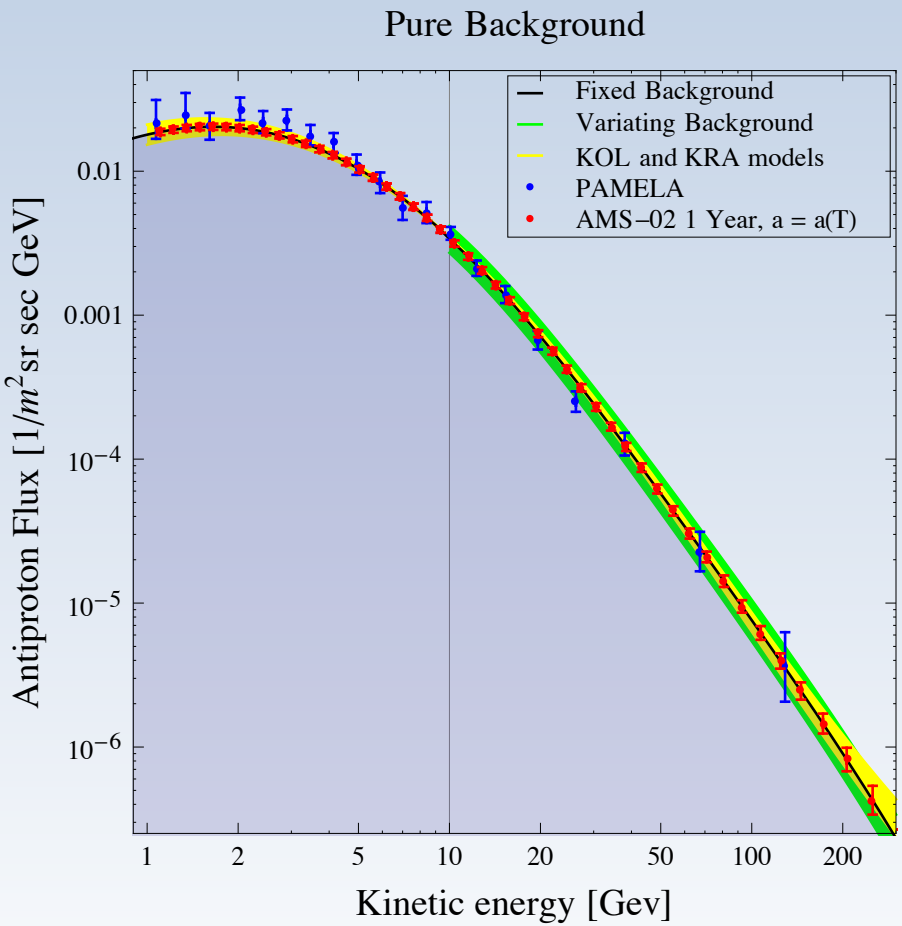


- Fixed Background
  $\phi_{\mathrm{fixed}}(T > 10\,\mathrm{GeV})$ : power law
- Variating background

$$\phi_{\mathrm{bkg}}(A, p; T) = AT^{p} \times \phi_{\mathrm{fixed}}(T)$$

$A \in [0.9, 1.1]$ and $p \in [-0.05, 0.05]$

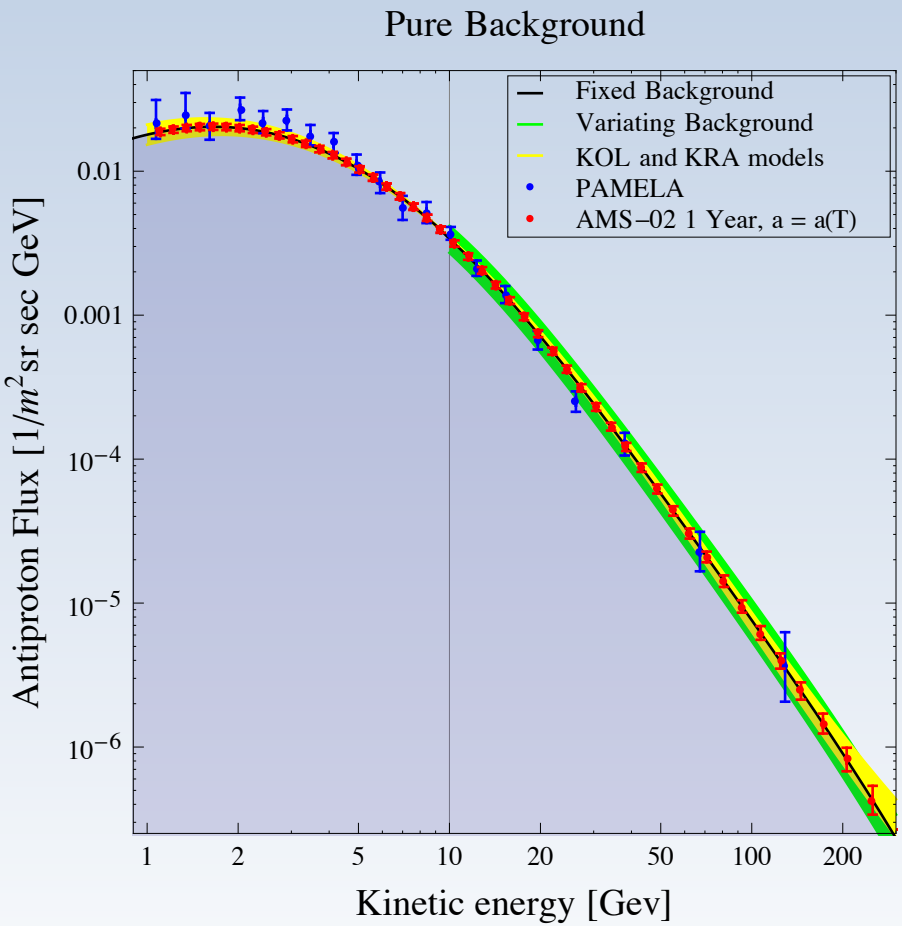


- Fixed Background
  $\phi_{\rm fixed}(T > 10\,{\rm GeV})$ : power law
- Variating background

$$\phi_{\rm bkg}(A, p; T) = AT^p \times \phi_{\rm fixed}(T)$$

$A \in [0.9, 1.1]$ and $p \in [-0.05, 0.05]$

- Flux with DM signal

$$\phi_{\rm tot}(m_{\rm DM}, \langle\sigma v\rangle; A, p) = \phi_{\rm DM}(m_{\rm DM}, \langle\sigma v\rangle) + \phi_{\rm bkg}(A, p)$$

$\Rightarrow$ Marginalization over $A$ and $p$

# Current Antiproton constraints from PAMELA for annihilating DM

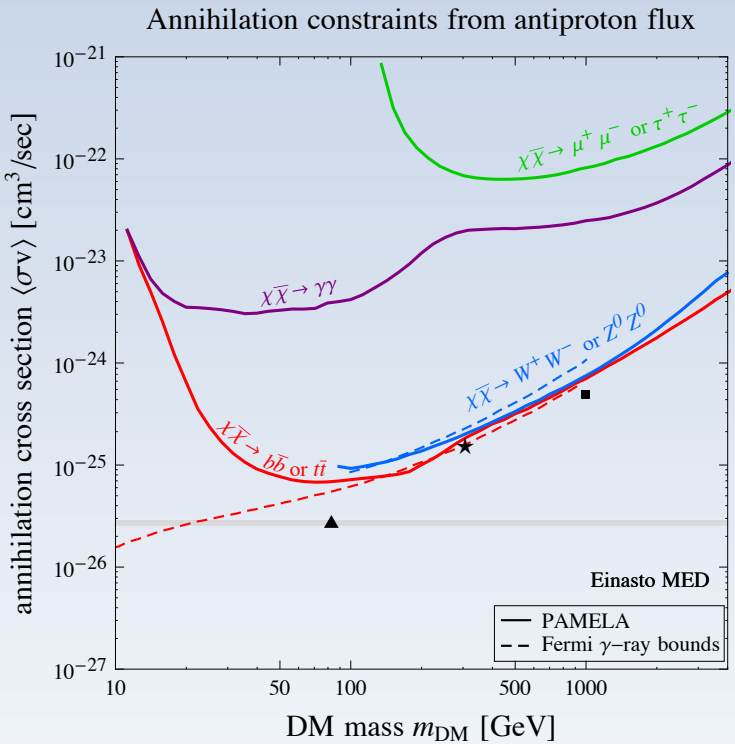


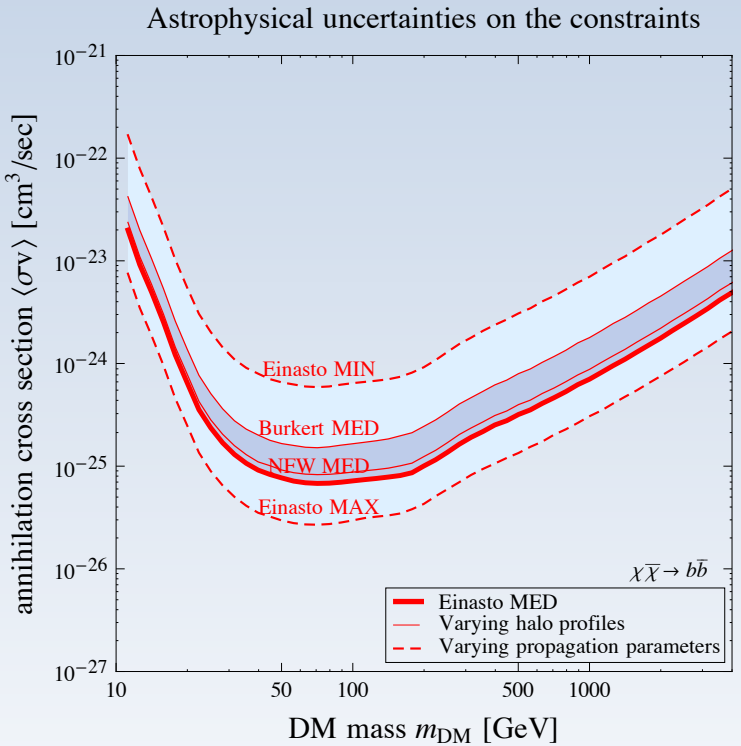

# Current Antiproton constraints from PAMELA for decaying DM

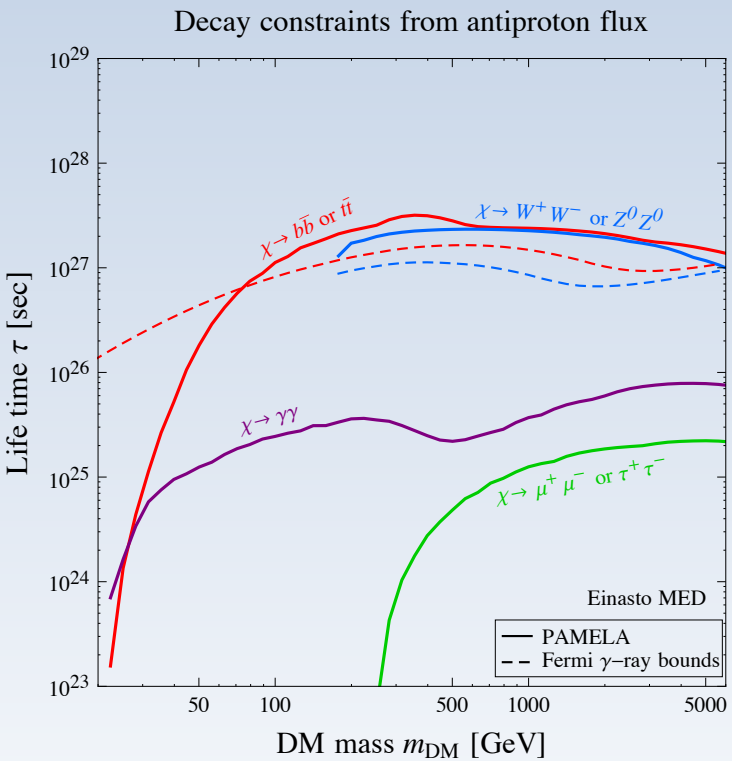


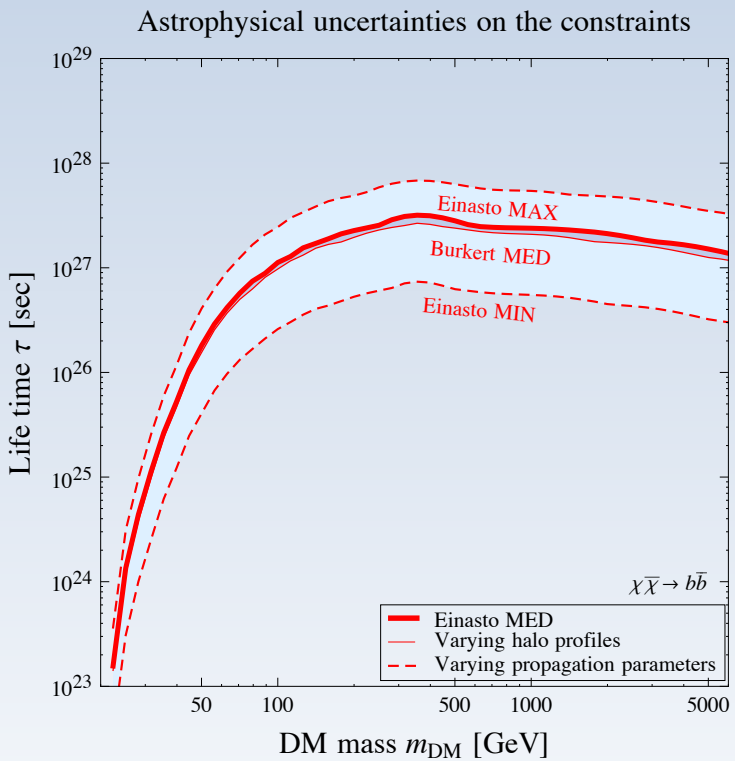

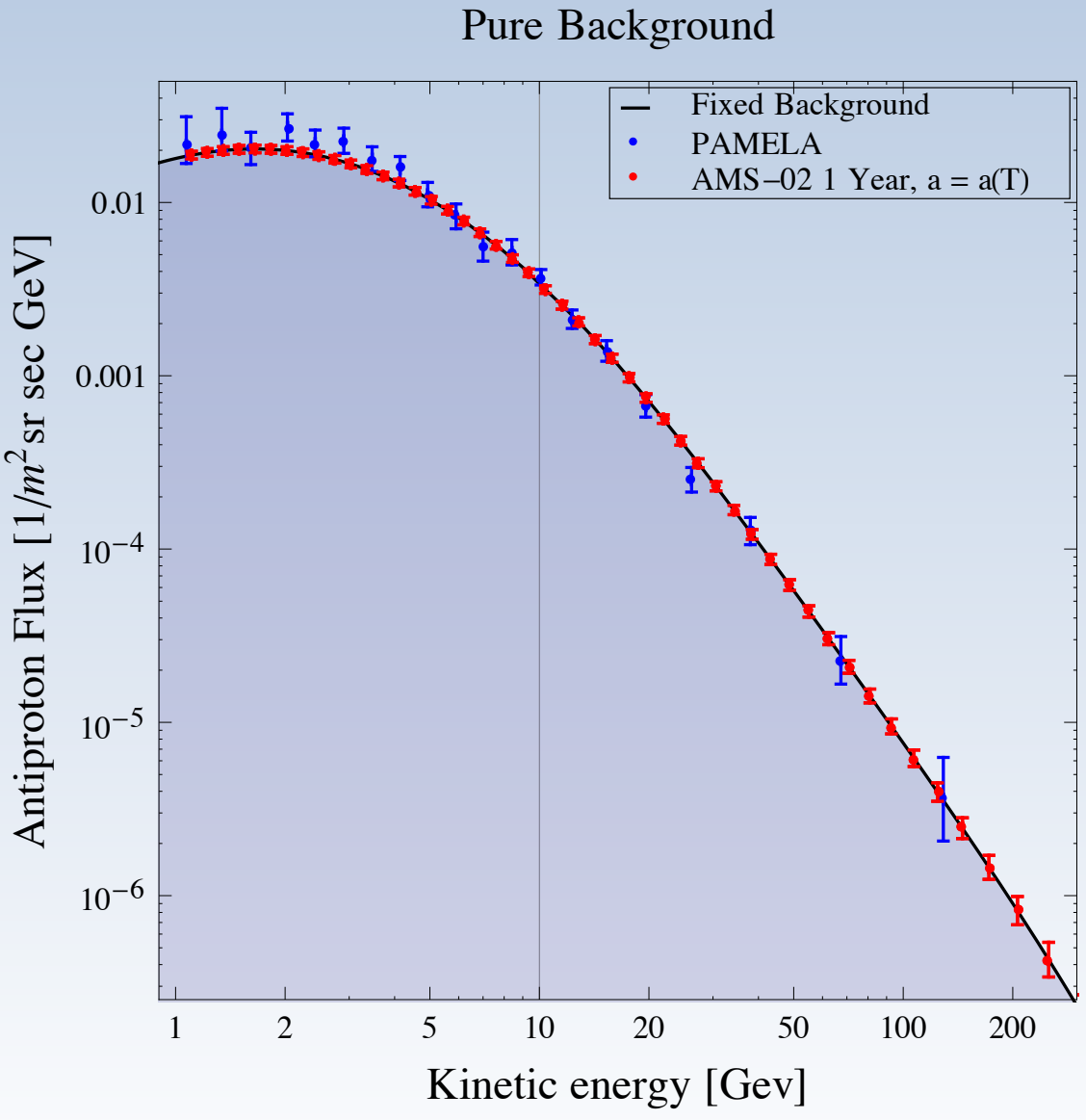
Pure Background
Fixed Background
PAMELA
AMS−02 1 Year, a = a(T)
Antiproton Flux [1/m² sr sec GeV]
0.01
0.001
10⁻⁴
10⁻⁵
10⁻⁶
1
2
5
10
20
50
100
200
Kinetic energy [Gev]

# Future sensitivities of AMS-02

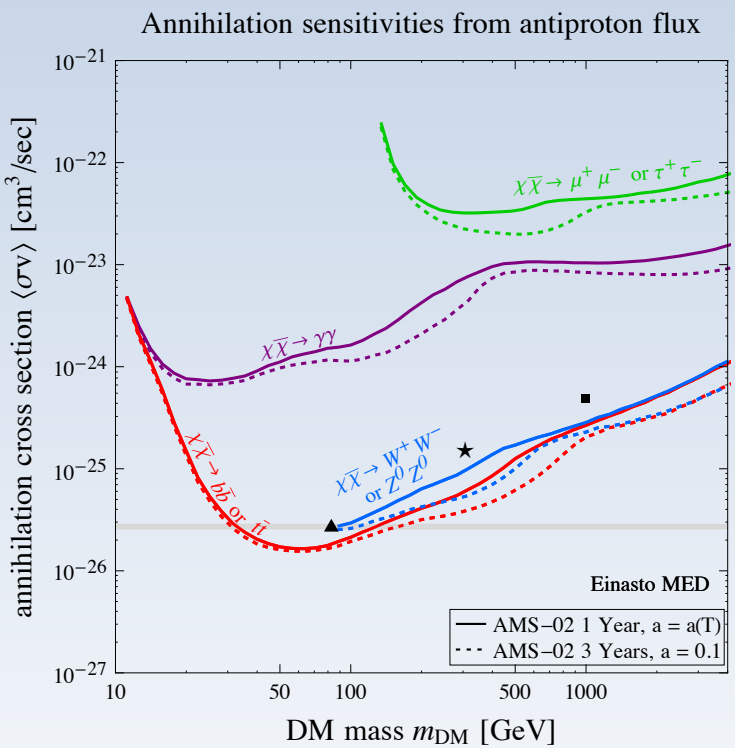


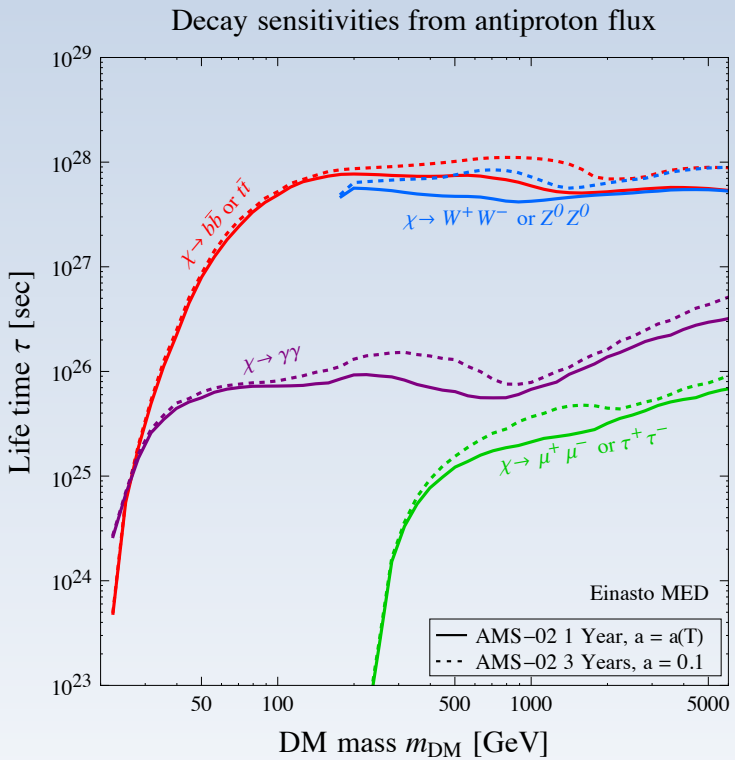

Study of three benchmark models :
Annihilation $\chi\chi \to b\bar{b}$, Einasto profile, MED propagation

Study of three benchmark models :
Annihilation $\chi\chi \to b\bar{b}$, Einasto profile, MED propagation

- $m_{\mathrm{DM}} = 85\,\mathrm{GeV}$ $\quad \langle \sigma v \rangle = 2.7 \times 10^{-26}\,\mathrm{cm}^3\,\mathrm{s}^{-1}$
  Thermal cross-section
  DM signal mainly below 10 $\mathrm{GeV}$

Study of three benchmark models :
Annihilation $\chi\chi \to b\bar{b}$, Einasto profile, MED propagation

▲ $m_{\mathrm{DM}} = 85\,\mathrm{GeV}$ $\langle\sigma v\rangle = 2.7 \times 10^{-26}\,\mathrm{cm}^3\,\mathrm{s}^{-1}$
Thermal cross-section
DM signal mainly below 10 $\mathrm{GeV}$

★ $m_{\mathrm{DM}} = 300\,\mathrm{GeV}$ $\langle\sigma v\rangle = 1.5 \times 10^{-25}\,\mathrm{cm}^3\,\mathrm{s}^{-1}$
Cross-section at the limit of exclusion
DM signal in the sensitivity of $\mathrm{AMS\text{-}02}$

Study of three benchmark models :
Annihilation $\chi\chi \to b\bar{b}$, Einasto profile, MED propagation

▲ $m_{\mathrm{DM}} = 85\,\mathrm{GeV}$ $\langle\sigma v\rangle = 2.7 \times 10^{-26}\,\mathrm{cm}^3\,\mathrm{s}^{-1}$
Thermal cross-section
DM signal mainly below 10 $\mathrm{GeV}$

★ $m_{\mathrm{DM}} = 300\,\mathrm{GeV}$ $\langle\sigma v\rangle = 1.5 \times 10^{-25}\,\mathrm{cm}^3\,\mathrm{s}^{-1}$
Cross-section at the limit of exclusion
DM signal in the sensitivity of $\mathrm{AMS\text{-}02}$

■ $m_{\mathrm{DM}} = 1\,\mathrm{TeV}$ $\langle\sigma v\rangle = 5 \times 10^{-25}\,\mathrm{cm}^3\,\mathrm{s}^{-1}$
DM signal at high energies
Data has big uncertainties

★ $m_{\rm DM} = 300\,{\rm GeV}$ and $\langle\sigma v\rangle = 1.5 \times 10^{-25}\,{\rm cm}^3\,{\rm s}^{-1}$

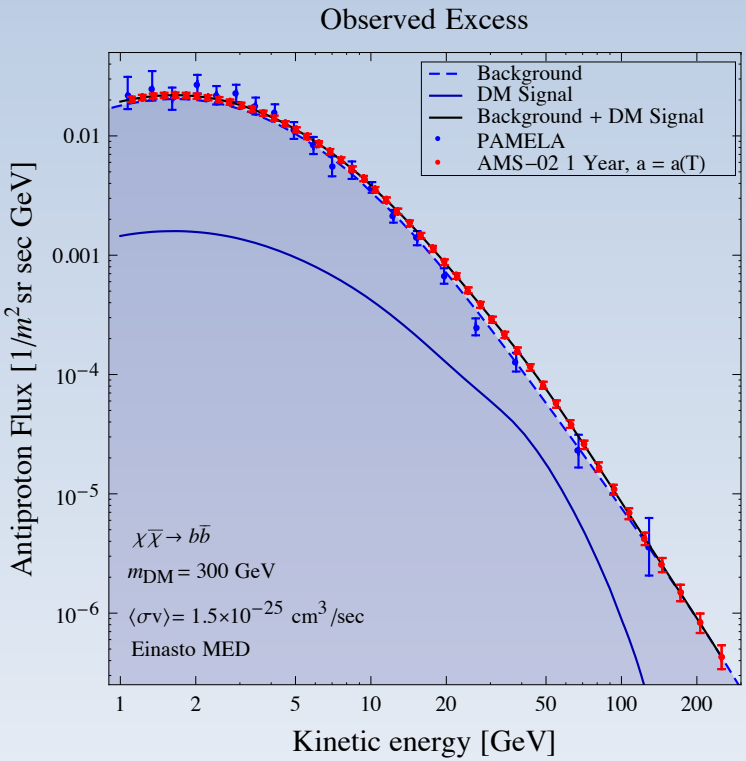

★ $m_{\rm DM} = 300\,{\rm GeV}$ and $\langle\sigma v\rangle = 1.5 \times 10^{-25}\,{\rm cm}^3\,{\rm s}^{-1}$

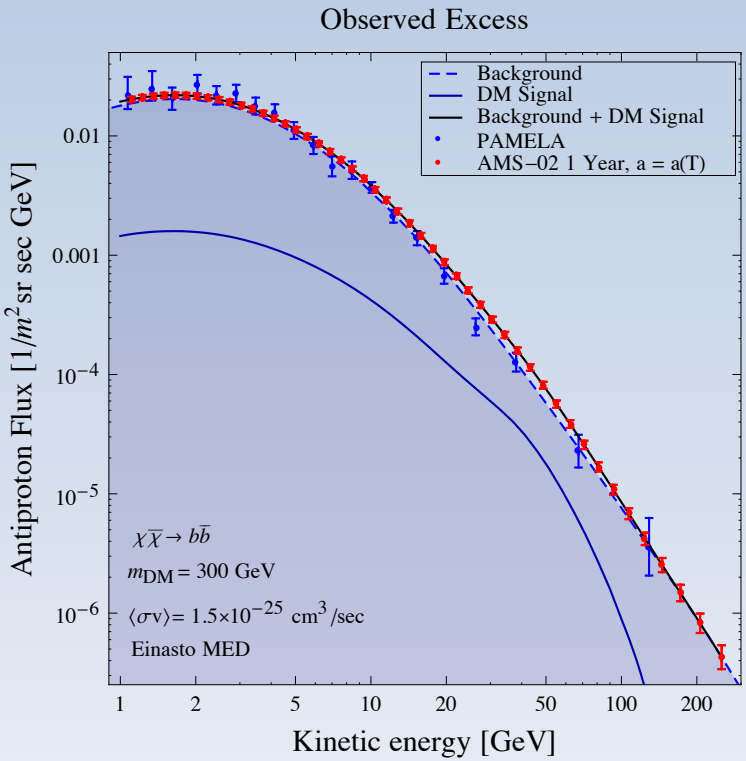


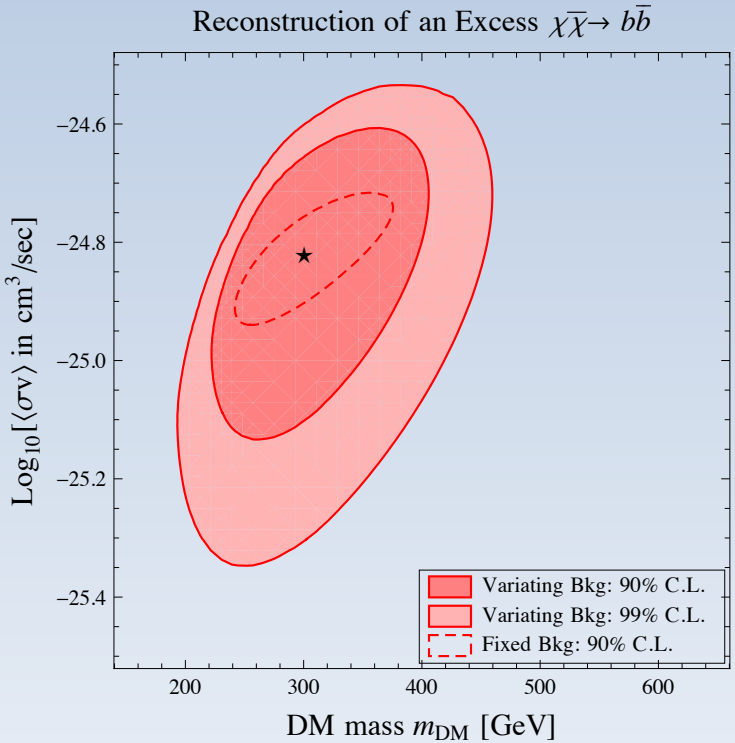

★ $m_{\rm DM} = 300\,{\rm GeV}$ and $\langle\sigma v\rangle = 1.5 \times 10^{-25}\,{\rm cm}^3\,{\rm s}^{-1}$

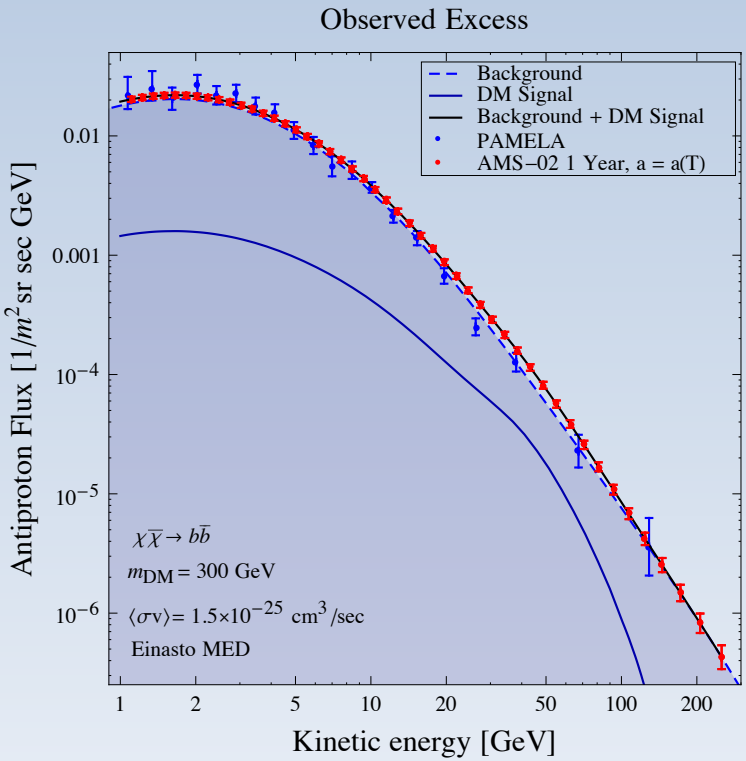


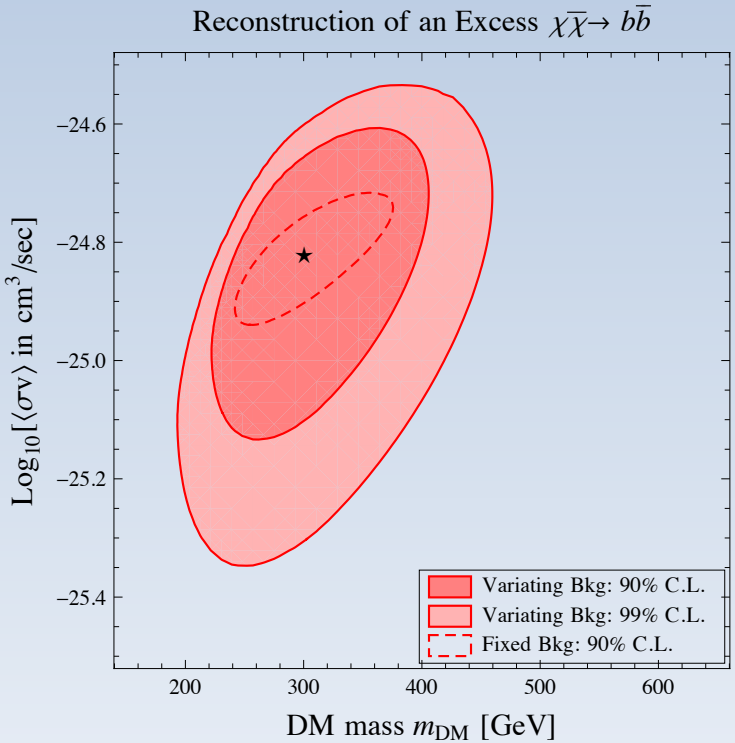


- Fixed background : degeneracy between $m^{-2}$ and $\langle\sigma v\rangle$

★ $m_{\mathrm{DM}} = 300\,\mathrm{GeV}$ and $\langle\sigma v\rangle = 1.5 \times 10^{-25}\,\mathrm{cm}^3\,\mathrm{s}^{-1}$

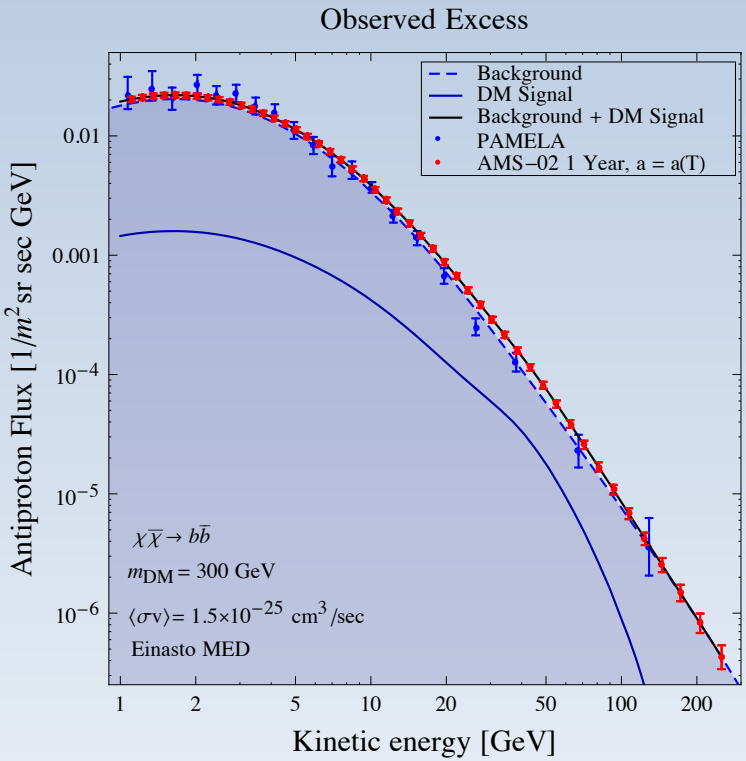


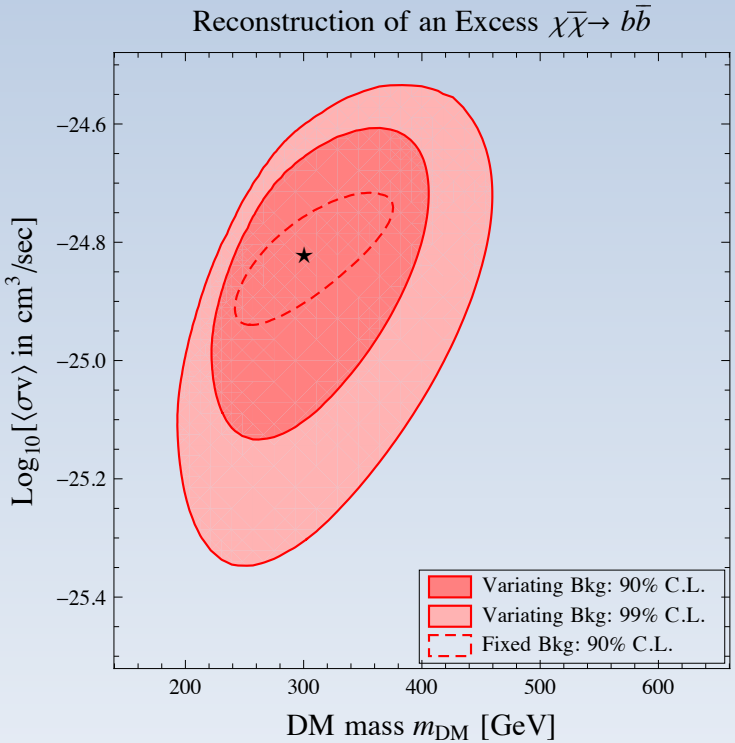


- Fixed background : degeneracy between $m^{-2}$ and $\langle\sigma v\rangle$
- $m_{DM}$ determined with 50% of its value
- $\langle\sigma v\rangle$ determined within an order of magnitude

★ $m_{\rm DM} = 300\,{\rm GeV}$ and $\langle\sigma v\rangle = 1.5 \times 10^{-25}\,{\rm cm}^3\,{\rm s}^{-1}$

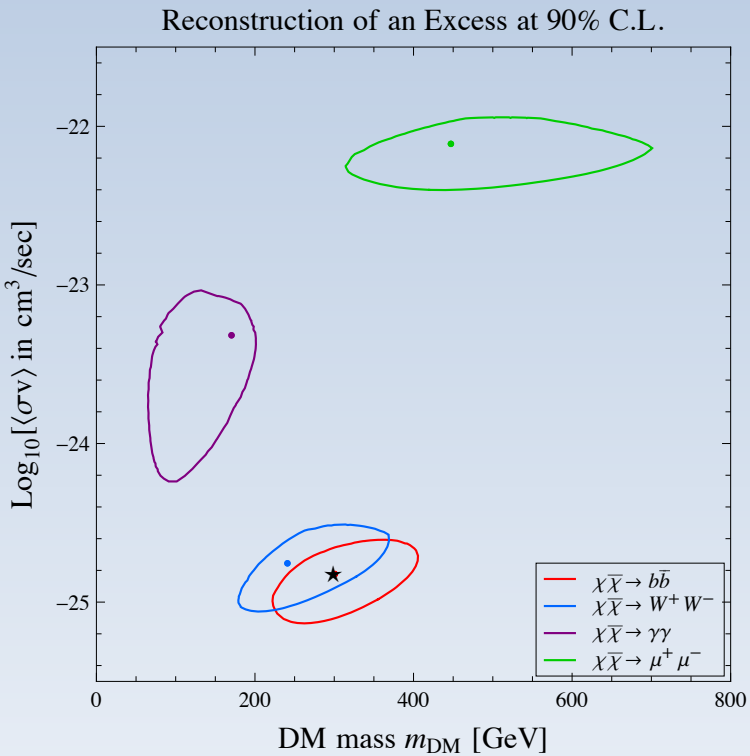


| Fixed annihilation channel (true signal : **100% $b\bar{b}$**) | mass $m_{\rm DM}$ [GeV] | cross-section $\langle\sigma v\rangle$ [cm$^3$s$^{-1}$] | $\Delta\chi^2$ with respect to a pure background |
|---|---|---|---|
| $\chi\chi \to b\bar{b}$ | 300 | $1.5 \times 10^{-25}$ | −21.0 |
| $\chi\chi \to W^+W^-$ | 240 | $1.9 \times 10^{-25}$ | −19.7 |
| $\chi\chi \to \gamma\gamma$ | 169 | $4.8 \times 10^{-24}$ | −9.8 |
| $\chi\chi \to \mu^+\mu^-$ | 447 | $7.6 \times 10^{-23}$ | −19.2 |

★ $m_{\rm DM} = 300\,{\rm GeV}$ and $\langle\sigma v\rangle = 1.5 \times 10^{-25}\,{\rm cm}^3\,{\rm s}^{-1}$

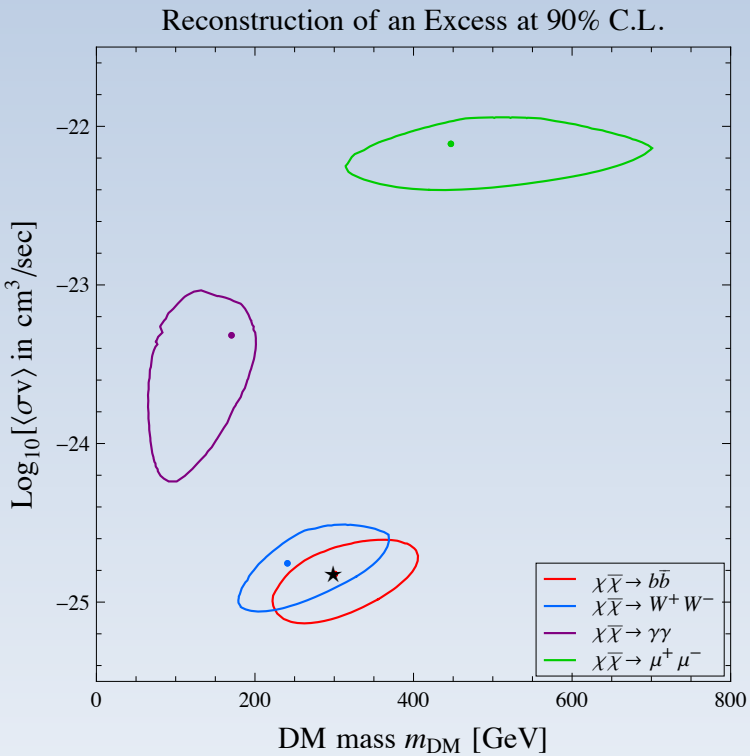


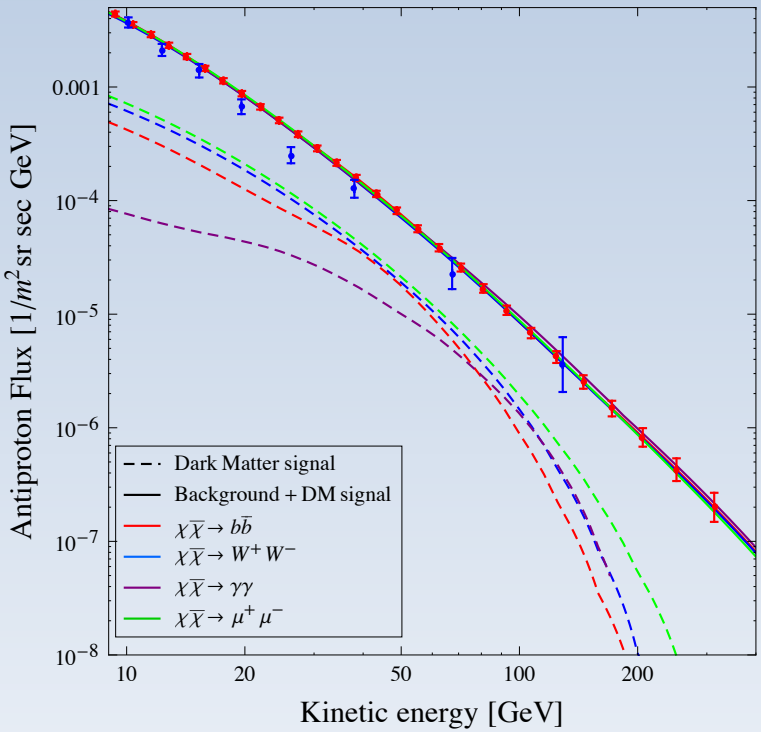


| Fixed annihilation channel (true signal : **100% $b\bar{b}$**) | mass $m_{\rm DM}$ [GeV] | cross-section $\langle\sigma v\rangle$ [cm$^3$s$^{-1}$] | $\Delta\chi^2$ with respect to a pure background |
|---|---|---|---|
| $\chi\chi \to b\bar{b}$ | 300 | $1.5 \times 10^{-25}$ | $-21.0$ |
| $\chi\chi \to W^+W^-$ | 240 | $1.9 \times 10^{-25}$ | $-19.7$ |
| $\chi\chi \to \gamma\gamma$ | 169 | $4.8 \times 10^{-24}$ | $-9.8$ |
| $\chi\chi \to \mu^+\mu^-$ | 447 | $7.6 \times 10^{-23}$ | $-19.2$ |

# New annihilation signal : **40% $b\bar{b}$ + 60% $W^+W^-$**

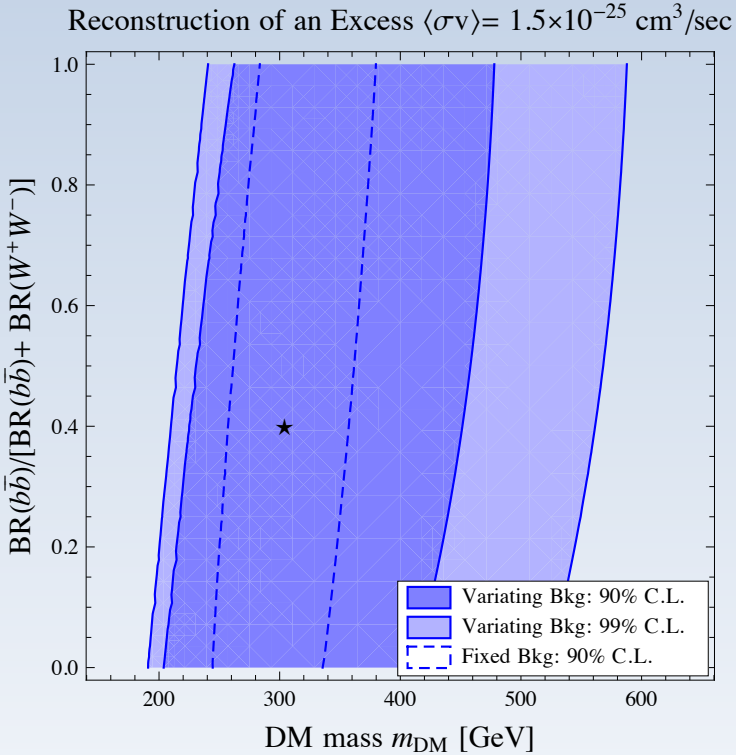


| Fixed cross-section $\langle\sigma v\rangle$ [cm$^3$s$^{-1}$] (true signal : **40% $b\bar{b}$ + 60% $W^+W^-$**) | mass $m_{\rm DM}$ [GeV] | relative branching ratio | $\Delta\chi^2$ with respect to a pure background |
|---|---|---|---|
| $1.5 \times 10^{-25}$ | 300 | 0.4 | −13.0 |

▲ $m_{\mathrm{DM}} = 85\,\mathrm{GeV}$ and $\langle \sigma v \rangle = 2.7 \times 10^{-26}\,\mathrm{cm}^3\,\mathrm{s}^{-1}$

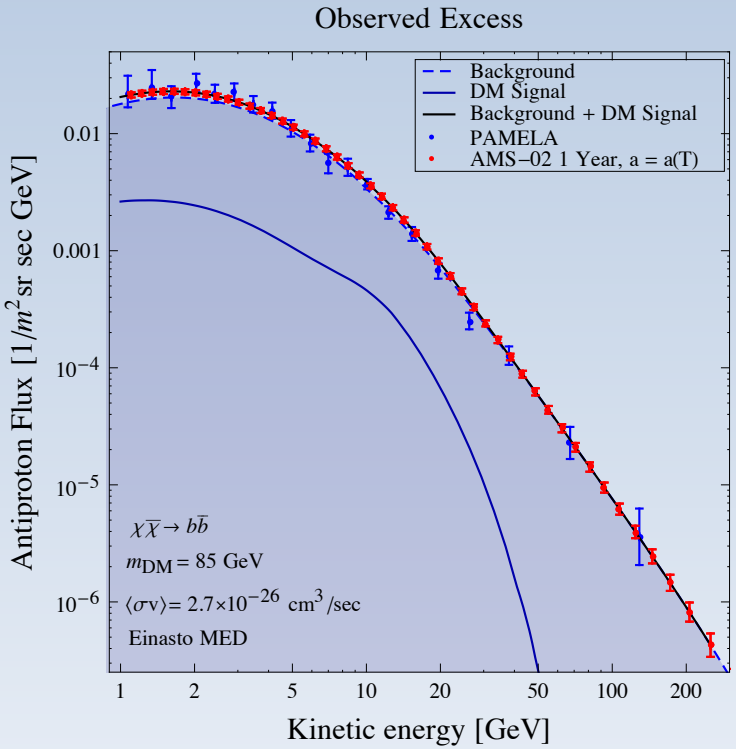

▲ $m_{\mathrm{DM}} = 85\,\mathrm{GeV}$ and $\langle \sigma v \rangle = 2.7 \times 10^{-26}\,\mathrm{cm}^3\,\mathrm{s}^{-1}$

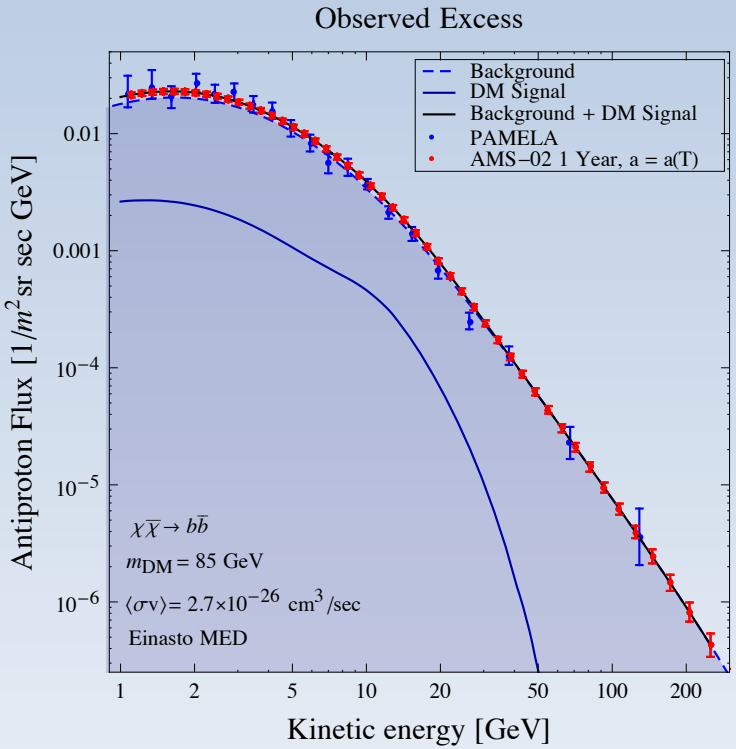


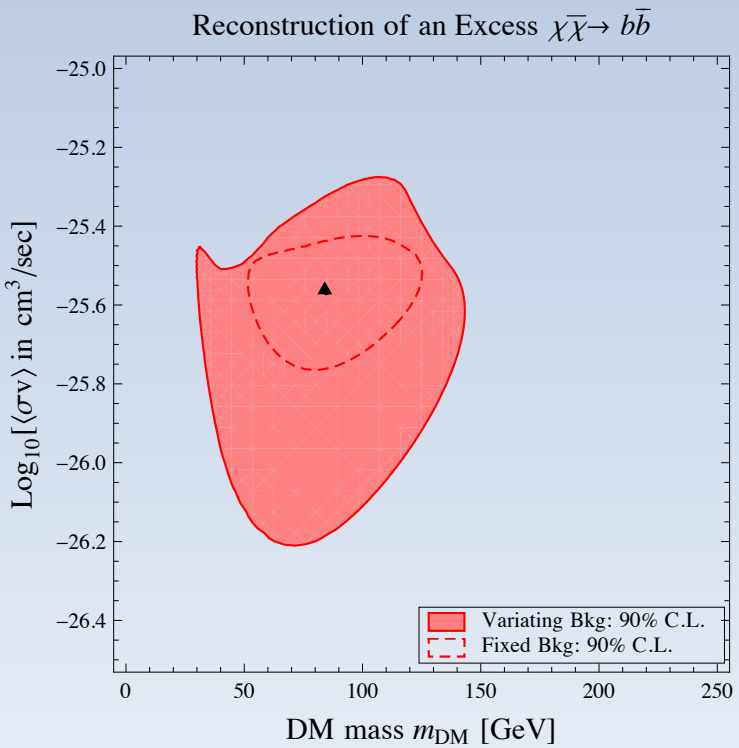

▲ $m_{\rm DM} = 85\,{\rm GeV}$ and $\langle\sigma v\rangle = 2.7 \times 10^{-26}\,{\rm cm}^3\,{\rm s}^{-1}$

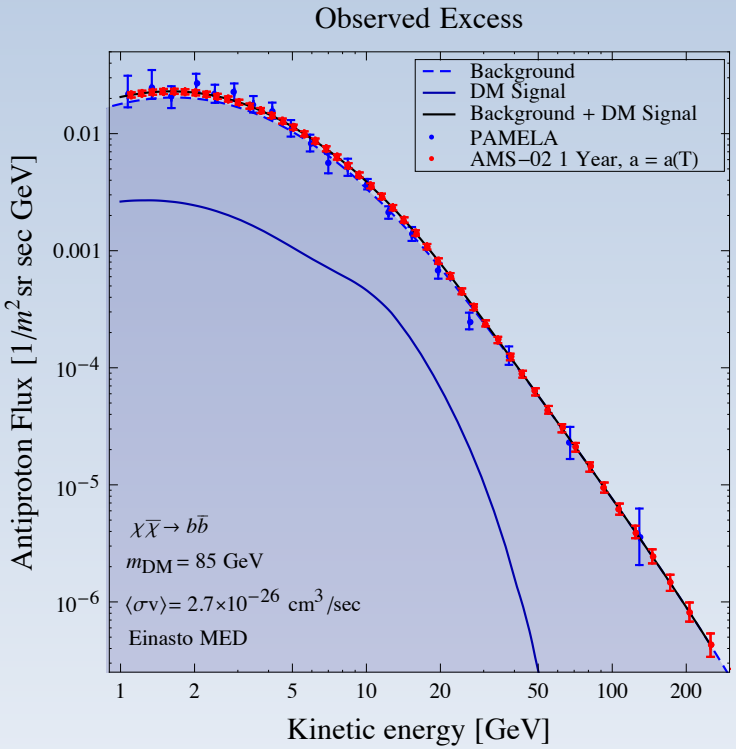


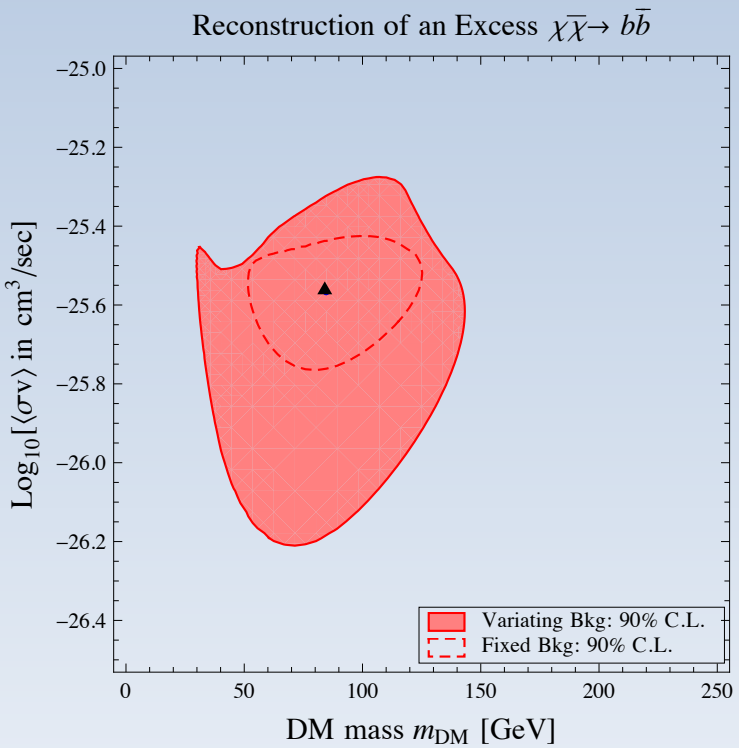


- Unusual shape, because of the 10 GeV cut

▲ $m_{\rm DM} = 85\,{\rm GeV}$ and $\langle\sigma v\rangle = 2.7 \times 10^{-26}\,{\rm cm}^3\,{\rm s}^{-1}$

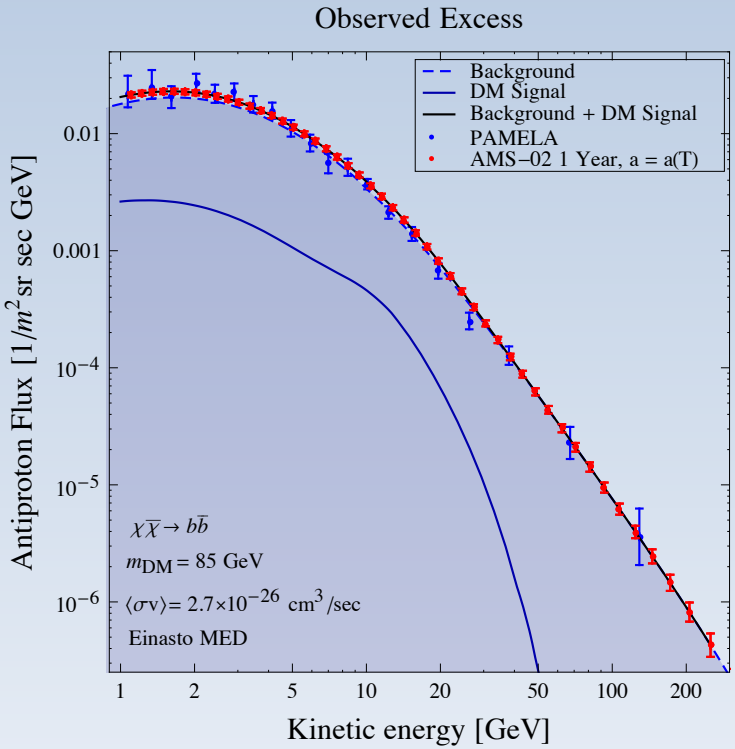


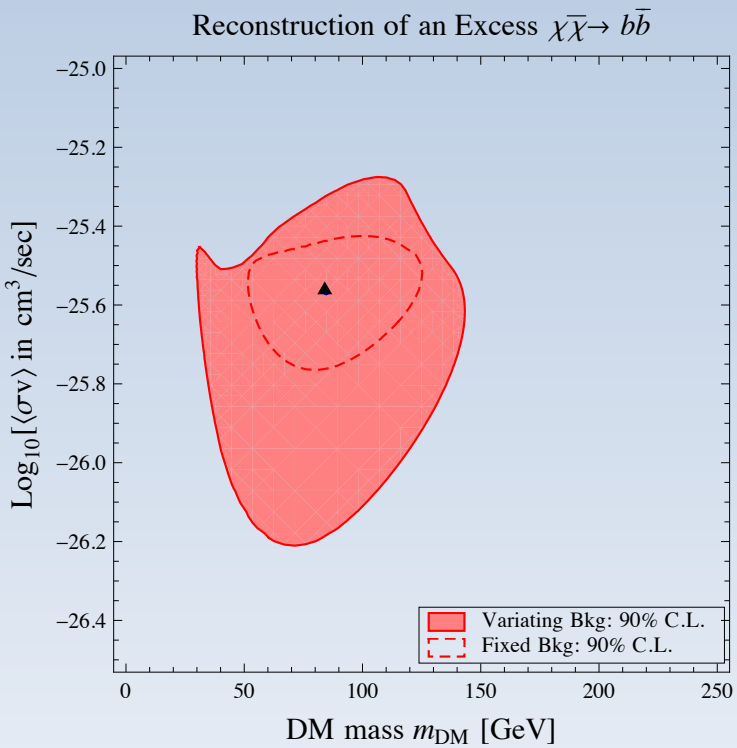


- Unusual shape, because of the 10 $\rm GeV$ cut
- 99% C.L. contour would extend artificially to low masses
- Points in the 99% C.L. contour prefer a pure background

▲ $m_{\rm DM} = 85\,{\rm GeV}$ and $\langle\sigma v\rangle = 2.7 \times 10^{-26}\,{\rm cm}^3\,{\rm s}^{-1}$

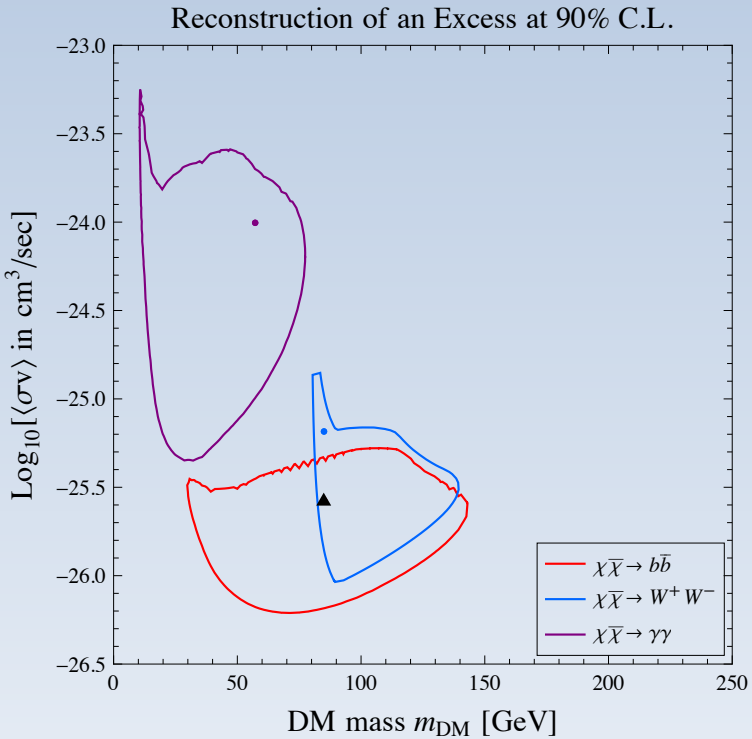


| Fixed annihilation channel (true signal : **100% $b\bar{b}$**) | mass $m_{\rm DM}$ [GeV] | cross-section $\langle\sigma v\rangle$ [$\rm cm^3 s^{-1}$] | $\Delta\chi^2$ with respect to a pure background |
|---|---|---|---|
| $\chi\chi \to b\bar{b}$ | 84.9 | $2.7 \times 10^{-26}$ | −10.5 |
| $\chi\chi \to W^+W^-$ | 84.8 | $6.6 \times 10^{-26}$ | −10.3 |
| $\chi\chi \to \gamma\gamma$ | 57.4 | $1.0 \times 10^{-24}$ | −5.7 |

▲ $m_{\rm DM} = 85\,{\rm GeV}$ and $\langle\sigma v\rangle = 2.7 \times 10^{-26}\,{\rm cm}^3\,{\rm s}^{-1}$

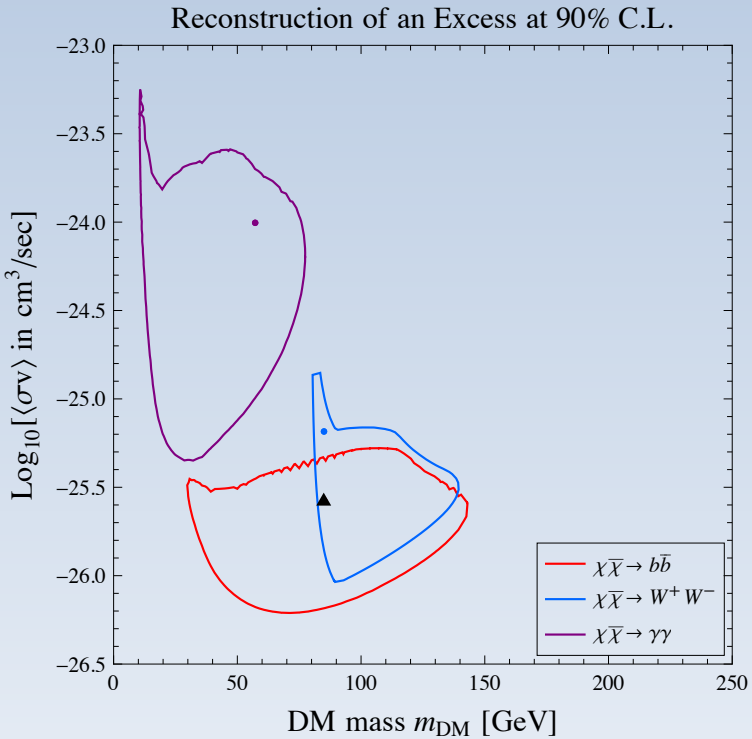


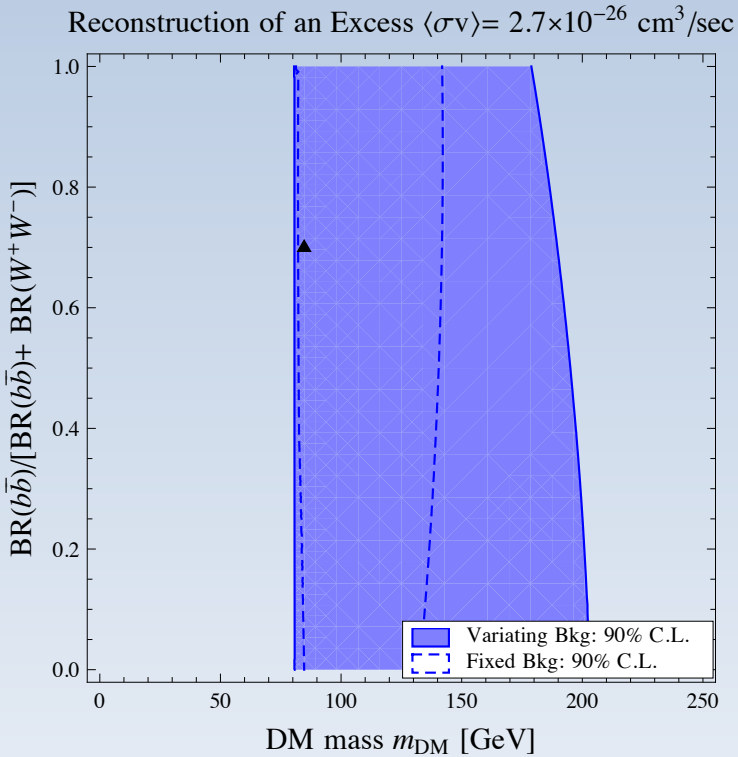


| Fixed annihilation channel (true signal : **100% $b\bar{b}$**) | mass $m_{\rm DM}$ [GeV] | cross-section $\langle\sigma v\rangle$ [$\rm cm^3 s^{-1}$] | $\Delta\chi^2$ with respect to a pure background |
|---|---|---|---|
| $\chi\chi \to b\bar{b}$ | 84.9 | $2.7 \times 10^{-26}$ | −10.5 |
| $\chi\chi \to W^+W^-$ | 84.8 | $6.6 \times 10^{-26}$ | −10.3 |
| $\chi\chi \to \gamma\gamma$ | 57.4 | $1.0 \times 10^{-24}$ | −5.7 |

| Fixed cross-section $\langle\sigma v\rangle$ [$\rm cm^3 s^{-1}$] (true signal : **70% $b\bar{b}$ + 30% $W^+W^-$**) | mass $m_{\rm DM}$ [GeV] | relative branching ratio | $\Delta\chi^2$ with respect to a pure background |
|---|---|---|---|
| $2.7 \times 10^{-26}$ | 84.9 | 0.7 | −5.4 |

- $m_{\rm DM} = 1\,\mathrm{TeV}$ and $\langle \sigma v \rangle = 5 \times 10^{-25}\,\mathrm{cm}^3\,\mathrm{s}^{-1}$

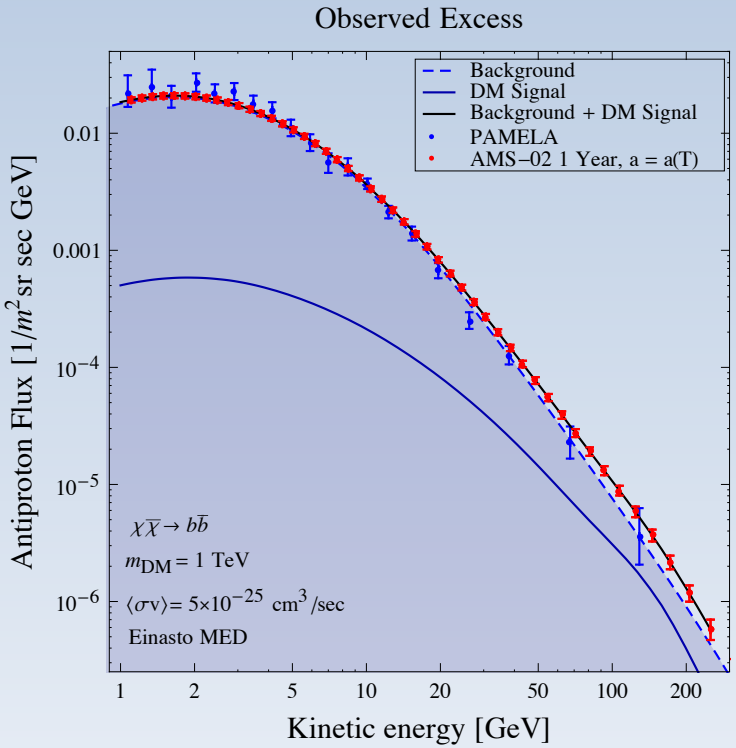

- $m_{\rm DM} = 1\,\text{TeV}$ and $\langle \sigma v \rangle = 5 \times 10^{-25}\,\text{cm}^3\,\text{s}^{-1}$

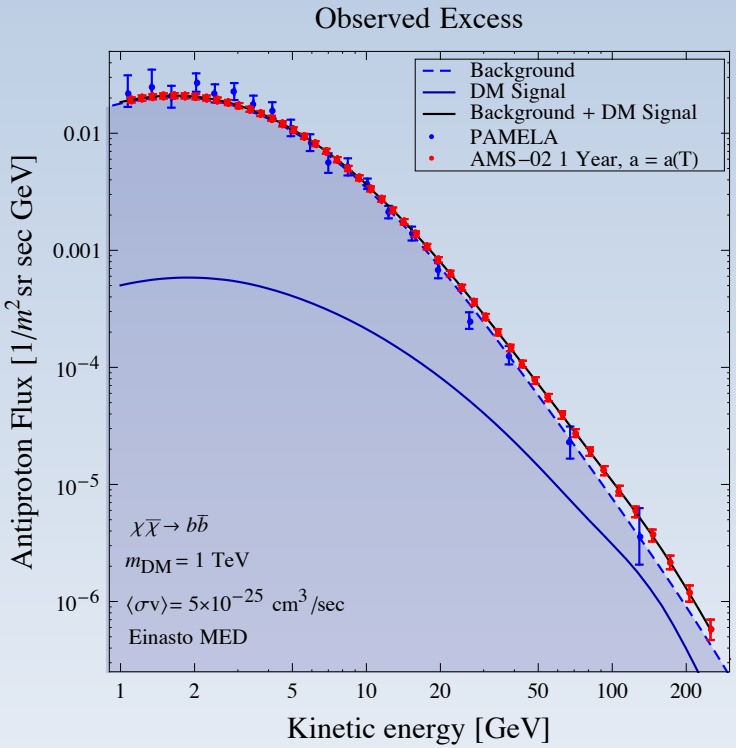


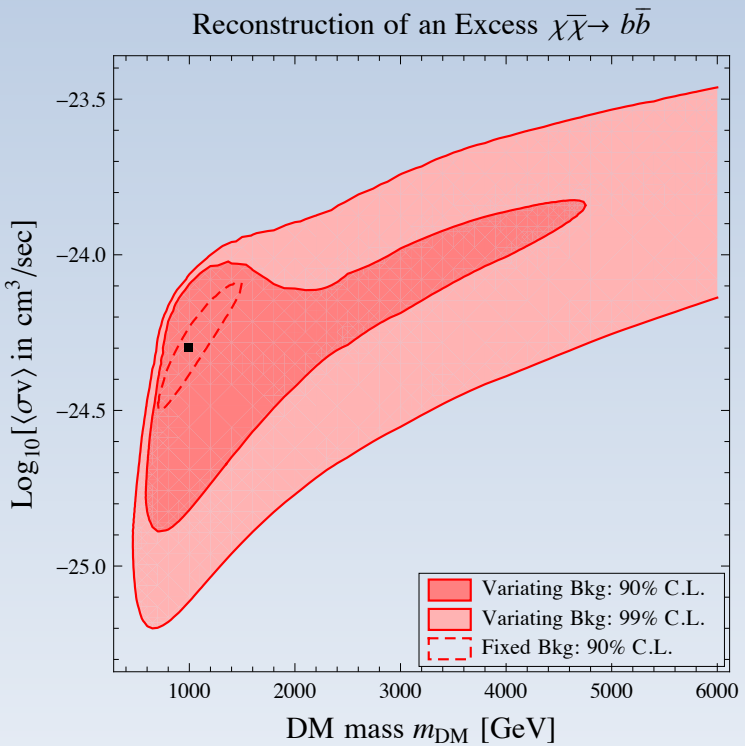

## $m_{\rm DM} = 1\,\mathrm{TeV}$ and $\langle \sigma v \rangle = 5 \times 10^{-25}\,\mathrm{cm}^3\,\mathrm{s}^{-1}$

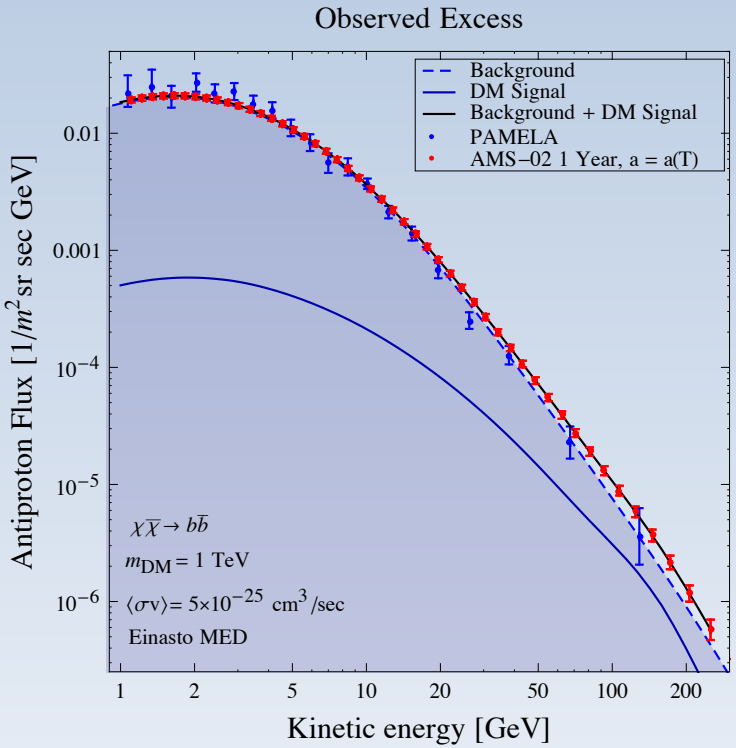


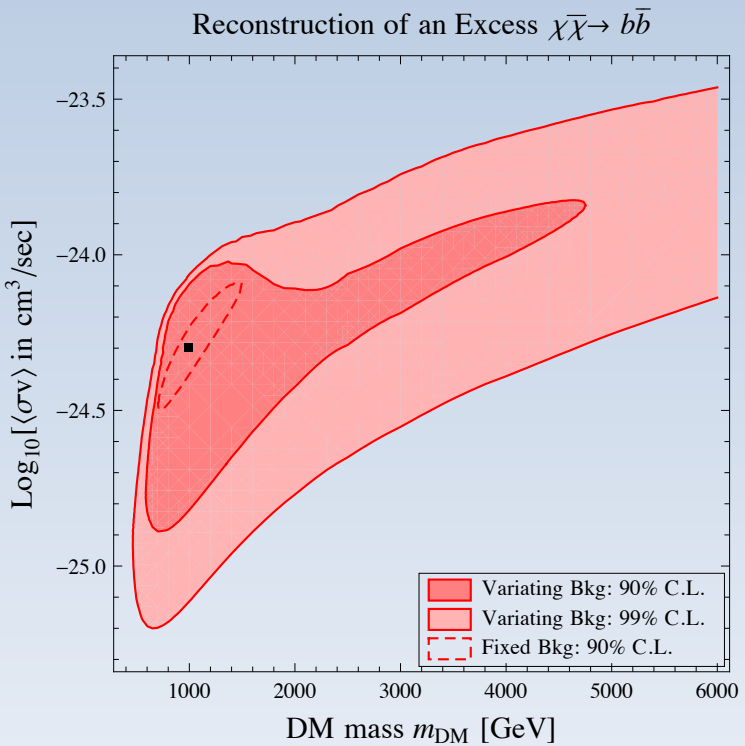


- 99% C.L. contour extends to high masses
- Any contribution with $m_{DM} > 1\,\mathrm{TeV}$ can fit the data at 99% C.L. with a cross-section large enough

- $m_{\rm DM} = 1\,\text{TeV}$ and $\langle\sigma v\rangle = 5 \times 10^{-25}\,\text{cm}^3\,\text{s}^{-1}$

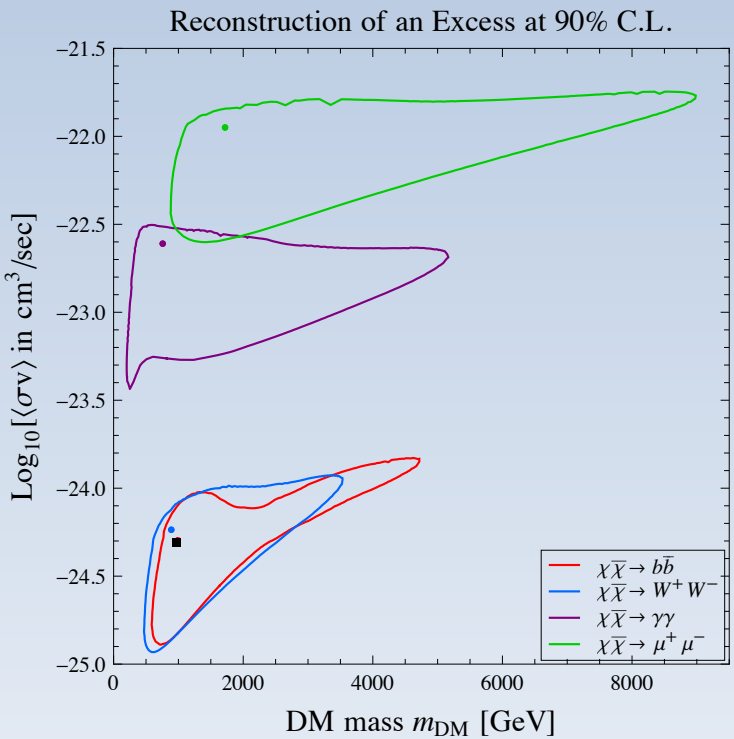


| Fixed annihilation channel (true signal : **100% $b\bar{b}$**) | mass $m_{\rm DM}$ [GeV] | cross-section $\langle\sigma v\rangle$ [$\text{cm}^3\text{s}^{-1}$] | $\Delta\chi^2$ with respect to a pure background |
|---|---|---|---|
| $\chi\chi \to b\bar{b}$ | 999 | $5 \times 10^{-25}$ | −15.7 |
| $\chi\chi \to W^+W^-$ | 886 | $5.8 \times 10^{-24}$ | −15.1 |
| $\chi\chi \to \gamma\gamma$ | 765 | $2.5 \times 10^{-22}$ | −14.5 |
| $\chi\chi \to \mu^+\mu^-$ | 1711 | $1.1 \times 10^{-22}$ | −14.8 |

- $m_{\rm DM} = 1\,{\rm TeV}$ and $\langle\sigma v\rangle = 5 \times 10^{-25}\,{\rm cm}^3\,{\rm s}^{-1}$

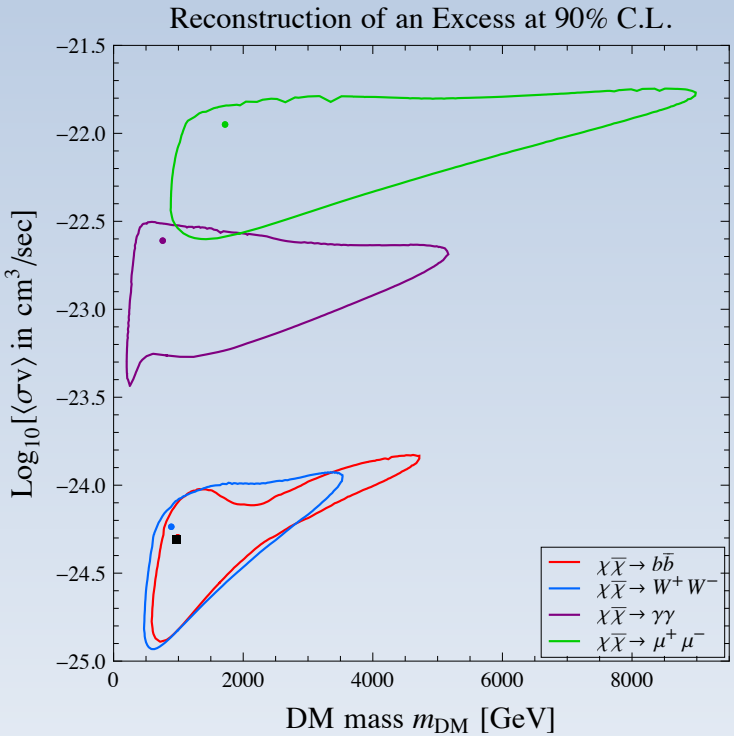


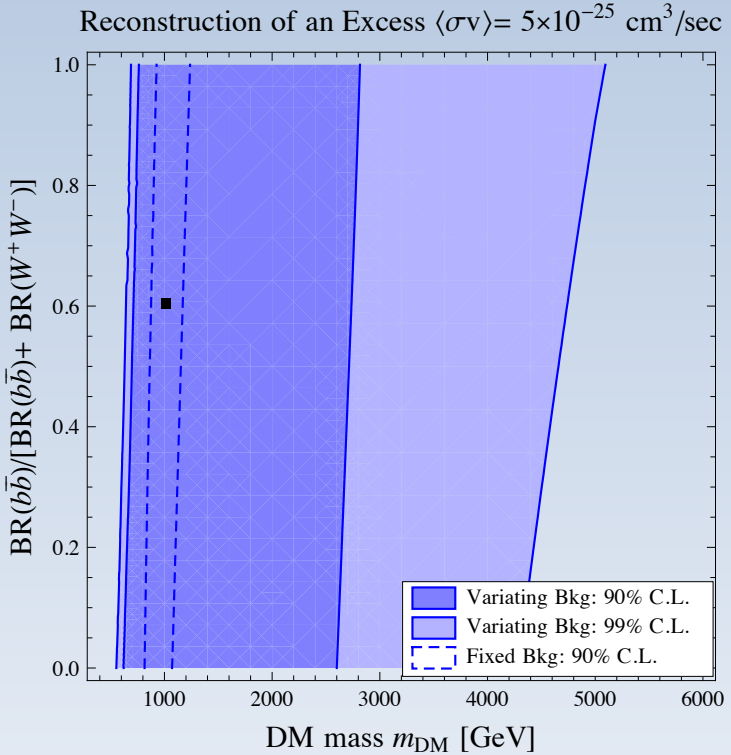


| Fixed annihilation channel (true signal : **100% $b\bar{b}$**) | mass $m_{\rm DM}$ [GeV] | cross-section $\langle\sigma v\rangle$ [$\rm cm^3 s^{-1}$] | $\Delta\chi^2$ with respect to a pure background |
|---|---|---|---|
| $\chi\chi \to b\bar{b}$ | 999 | $5 \times 10^{-25}$ | $-15.7$ |
| $\chi\chi \to W^+W^-$ | 886 | $5.8 \times 10^{-24}$ | $-15.1$ |
| $\chi\chi \to \gamma\gamma$ | 765 | $2.5 \times 10^{-22}$ | $-14.5$ |
| $\chi\chi \to \mu^+\mu^-$ | 1711 | $1.1 \times 10^{-22}$ | $-14.8$ |

| Fixed cross-section $\langle\sigma v\rangle$ [$\rm cm^3 s^{-1}$] (true signal : **60% $b\bar{b}$ + 40% $W^+W^-$**) | mass $m_{\rm DM}$ [GeV] | relative branching ratio | $\Delta\chi^2$ with respect to a pure background |
|---|---|---|---|
| $5 \times 10^{-25}$ | 999 | 0.6 | $-15.3$ |

- Current $\bar{p}$ constraints are competitive with gamma ray constraints from the FERMI satellite.
- Astrophysical uncertainties (halo profile, propagation) span over 1-2 orders of magnitude, background assumed to be a power law

- Current $\bar{p}$ constraints are competitive with gamma ray constraints from the FERMI satellite.
- Astrophysical uncertainties (halo profile, propagation) span over 1-2 orders of magnitude, background assumed to be a power law
- Assuming no signal is detected :
  - AMS-02 can improve the constraints by almost one order of magnitude
  - will probe the thermal value of annihilation cross-section for $m_{DM} \simeq 20 - 300\,\mathrm{GeV}$ for $b\bar{b}$ channel

- Current $\bar{p}$ constraints are competitive with gamma ray constraints from the FERMI satellite.
- Astrophysical uncertainties (halo profile, propagation) span over 1-2 orders of magnitude, background assumed to be a power law
- Assuming no signal is detected :
  - AMS-02 can improve the constraints by almost one order of magnitude
  - will probe the thermal value of annihilation cross-section for $m_{DM} \simeq 20 - 300\,\mathrm{GeV}$ for $b\bar{b}$ channel
- If an excess is measured :
  - Restricting to "traditional" hadronic channels :
    - $m_{DM}$ reconstructed within 50% for $m_{DM} \sim$ few hundred $\mathrm{GeV}$ (most favorable case)
    - $\langle \sigma v \rangle$ reconstructed within an order of magnitude
    - If several channels are open, relative branching ratios cannot be determined
  - If "exotic" annihilation channels open, no discrimination

Linear approximation of the rigidity resolution

$$r(T) = \frac{\Delta T}{T} = 0.0042 \times T + 0.1$$

The number of collected and reconstructed antiprotons in a bin $i$ centered around a kinetic energy $T_i$

$$N_i = \epsilon\, a(T_i)\, \phi(T_i)\, \Delta T_i\, \Delta t$$

| | |
|---|---|
| $\epsilon$ | the efficiency ($\epsilon = 1$ for protons), |
| $a$ | the geometrical acceptance of the apparatus, |
| $\phi$ | the antiproton flux, |
| $\Delta T$ | the width of the kinetic energy bin and |
| $\Delta t$ | the exposure time. |

Statistical error : $\Delta N = \sqrt{N} \Rightarrow \Delta\phi_i\,|_{stat} = \sqrt{\frac{\phi(T_i)}{\epsilon\, a(T_i)\, \Delta T_i\, \Delta t}}$

Systematic errors : $\Delta\phi_i\,|_{syst} = 0.05 \times \phi_i(T_i)$

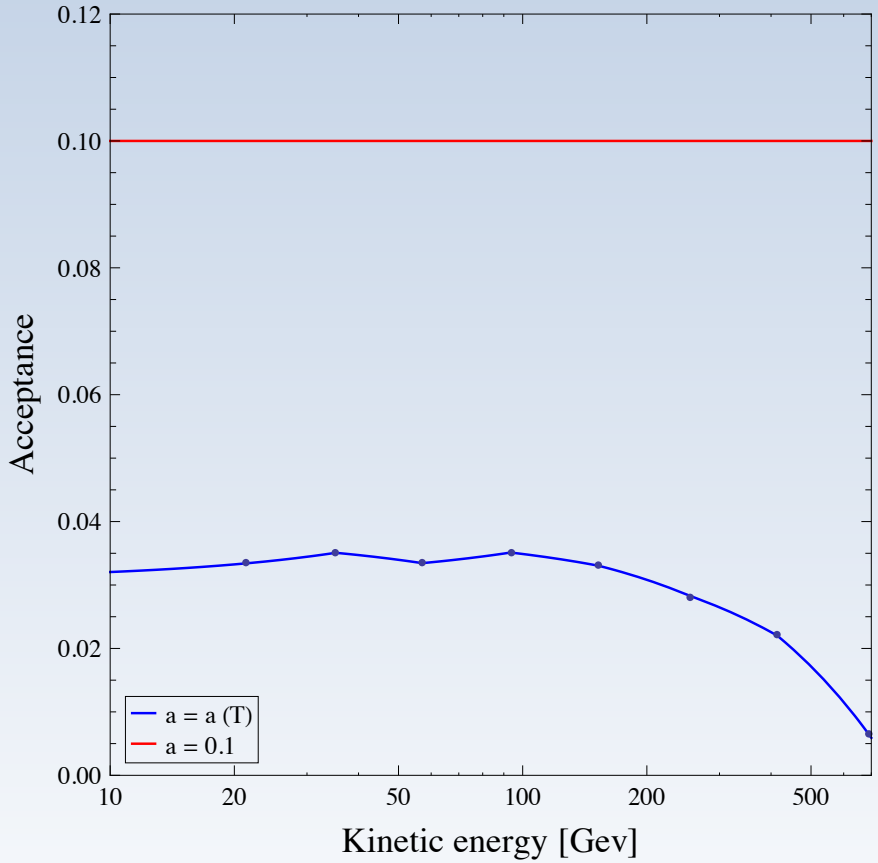


Two cases :

- Realistic
  $\Delta t = 1$ Year and $a = a(T)$,
- Idealistic
  $\Delta t = 3$ Years and $a = 0.1$

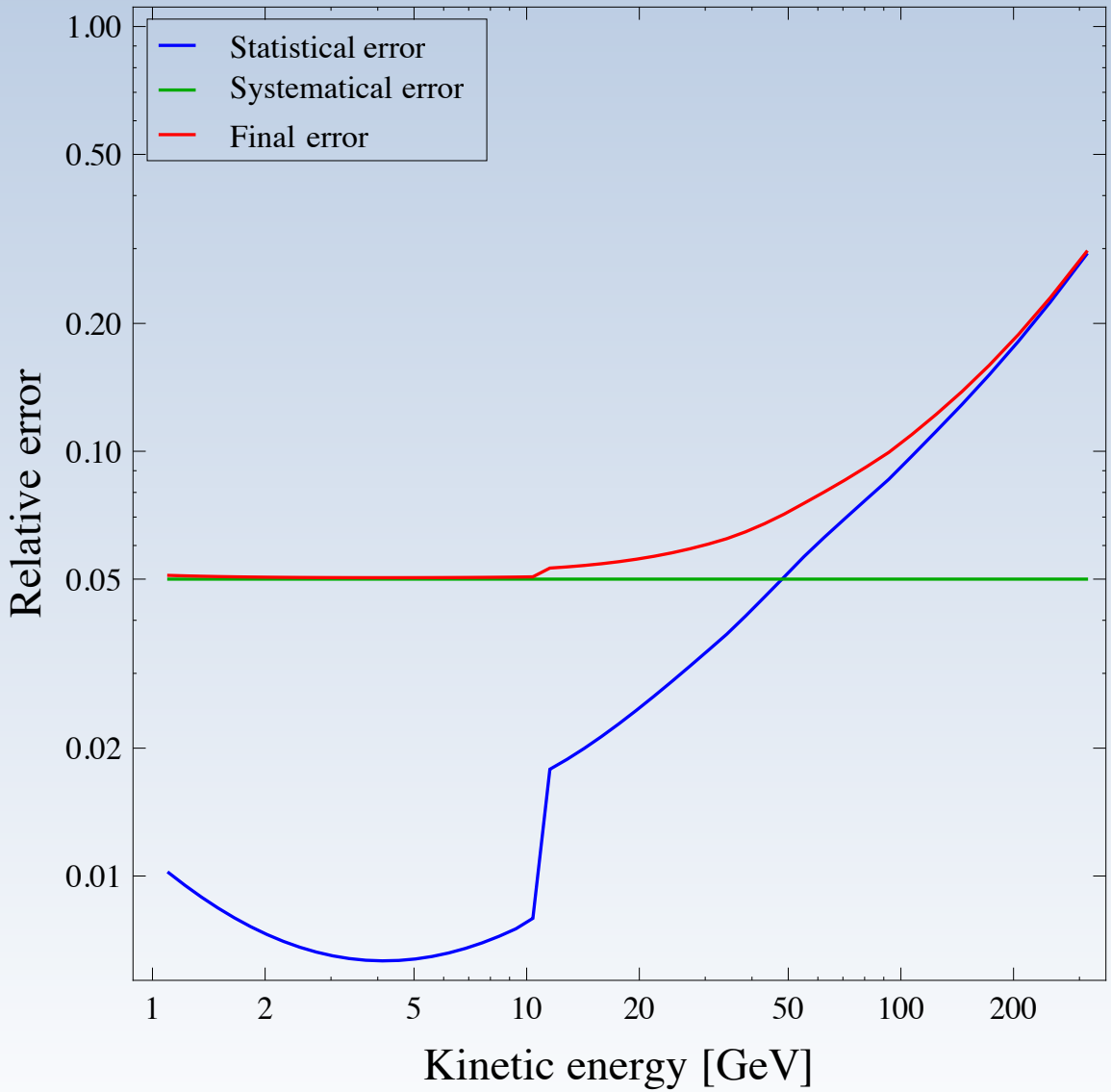
Statistical error
Systematical error
Final error
Relative error
1.00
0.50
0.20
0.10
0.05
0.02
0.01
1
2
5
10
20
50
100
200
Kinetic energy [GeV]

# Real signal : $\chi\chi \to b\bar{b}$, $m_{\rm DM} = 1\,\text{TeV}$ and $\langle\sigma v\rangle = 5 \times 10^{-25}$ cm$^3$s$^{-1}$

| Fixed annihilation channel (true signal : **100% b$\bar{\text{b}}$**) | mass $m_{\rm DM}$ [GeV] | cross-section $\langle\sigma v\rangle$ [cm$^3$s$^{-1}$] | $\Delta\chi^2$ with respect to a pure background |
|---|---|---|---|
| $\chi\chi \to b\bar{b}$ | 999 | $5 \times 10^{-25}$ | $-15.7$ |
| $\chi\chi \to W^+W^-$ | 886 | $5.8 \times 10^{-24}$ | $-15.1$ |
| $\chi\chi \to \gamma\gamma$ | 765 | $2.5 \times 10^{-22}$ | $-14.5$ |
| $\chi\chi \to \mu^+\mu^-$ | 1711 | $1.1 \times 10^{-22}$ | $-14.8$ |

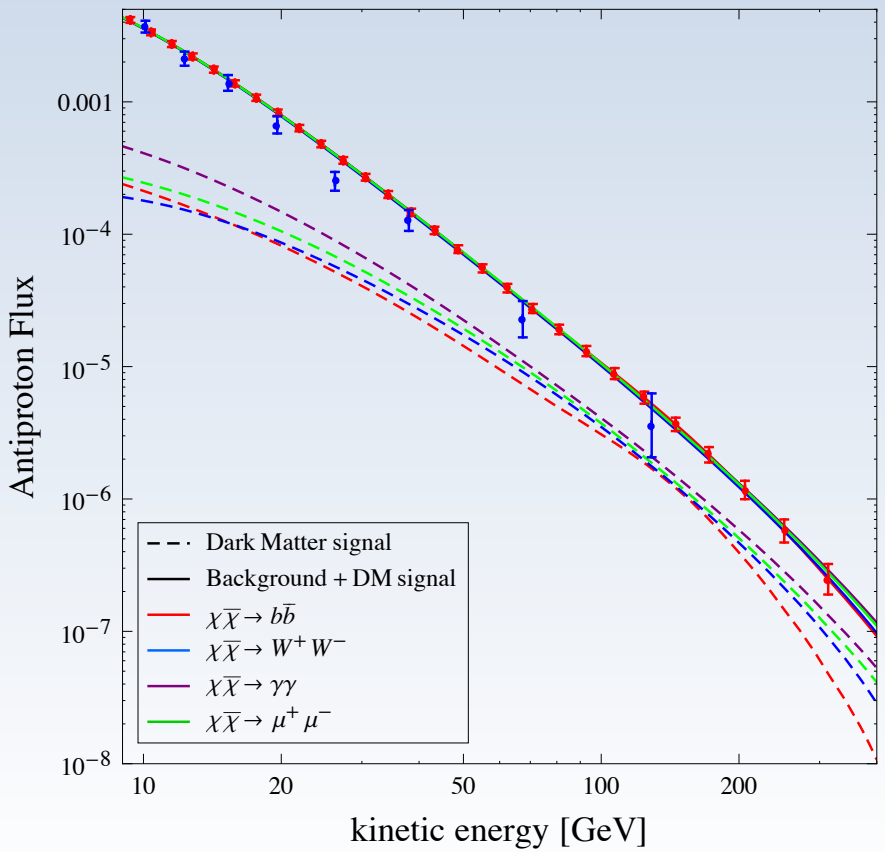

$$\rho_{\rm NFW}(r) = \rho_s \frac{r_s}{r}\left(1+\frac{r}{r_s}\right)^{-2} \qquad r_s = 24.42 \quad \rho_s = 0.184$$

$$\rho_{\rm Ein}(r) = \rho_s \exp\left\{-\frac{2}{\alpha}\left[\left(\frac{r}{r_s}\right)^{\alpha}-1\right]\right\} \qquad \alpha = 0.17 \quad r_s = 28.44 \quad \rho_s = 0.033$$

$$\rho_{\rm Bur}(r) = \frac{\rho_s}{(1+r/r_s)(1+(r/r_s)^2)} \qquad 1r_s = 2.67 \quad \rho_s = 0.712$$

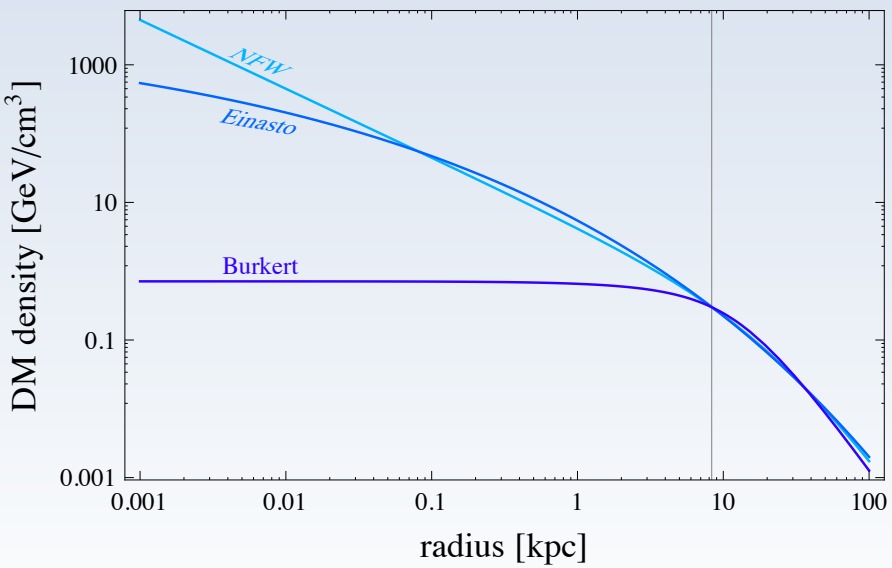

Diffusion equation for the number density of antiprotons per unit energy $f(t, \vec{x}, T)$ :

$$\frac{\partial f}{\partial t} - \mathcal{K} \cdot \nabla^2 f + \frac{\partial}{\partial z}(\mathrm{sign}(z) f V_{conv}) = Q - 2h\delta(z)(\Gamma_{\mathrm{ann}} + \Gamma_{\mathrm{non-ann}})f$$

| | |
|---|---|
| diffusion term | $\mathcal{K}(T) = \mathcal{K}_0 \beta \left(\frac{p}{\mathrm{GeV}}\right)^{\delta}$ |
| convective wind | $V_{\mathrm{conv}}$ |
| DM ann/decay source term | $Q$ |
| annihilation rate of $\bar{p}$ on $p$ | $\Gamma_{\mathrm{ann}}$ |
| interaction rate of $\bar{p}$ | $\Gamma_{\mathrm{non-ann}}$ |

| Model | $\delta$ | $\mathcal{K}_0$ [kpc$^2$/Myr] | $V_{\mathrm{conv}}$ [km/s] | $L$ [kpc] |
|---|---|---|---|---|
| MIN | 0.85 | 0.0016 | 13.5 | 1 |
| MED | 0.70 | 0.0112 | 12 | 4 |
| MAX | 0.46 | 0.0765 | 5 | 15 |

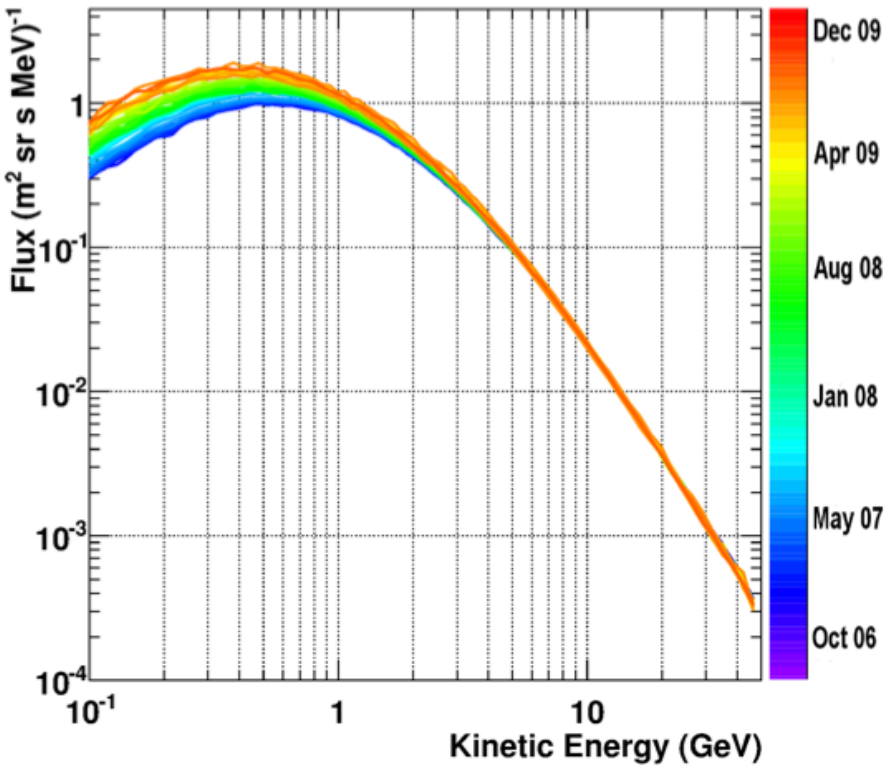


Fig. 4.— The evolution of the proton energy spectrum as particle intensities approached the period of minimum solar activity, from July 2006 (violet), to December 2009 (red). The region between the blue and red curves indicates the spread in proton fluxes during this time.

$$J_{\oplus}(K) = J_{\mathrm{LIS}}(K + \phi\frac{Z}{A})\frac{K(K+2\,m)}{(K+m+\phi\frac{Z}{A})^2 - m^2}.$$

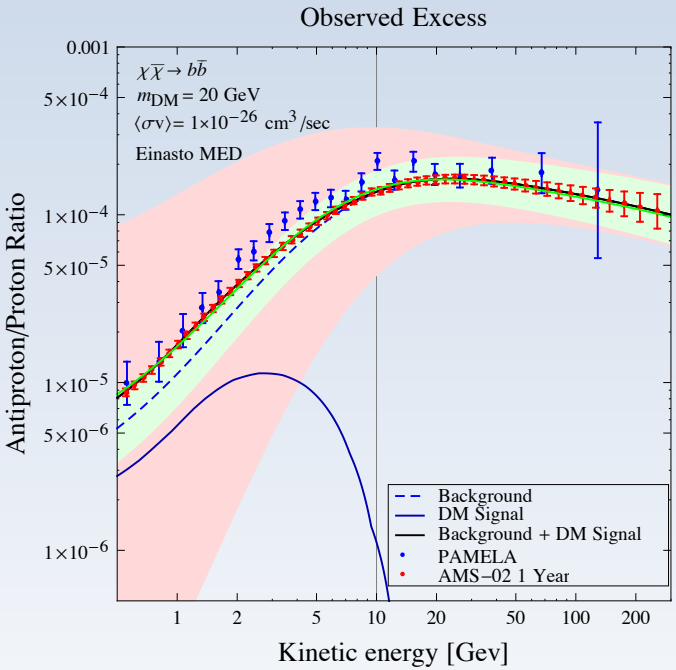


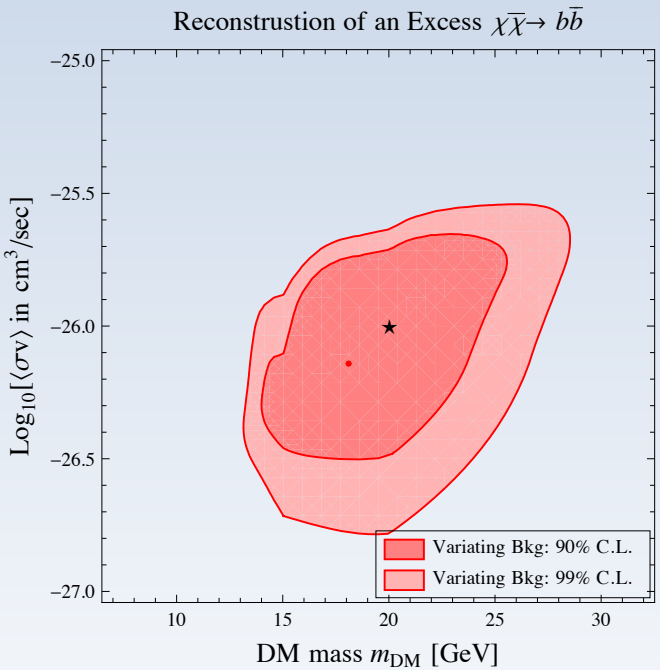

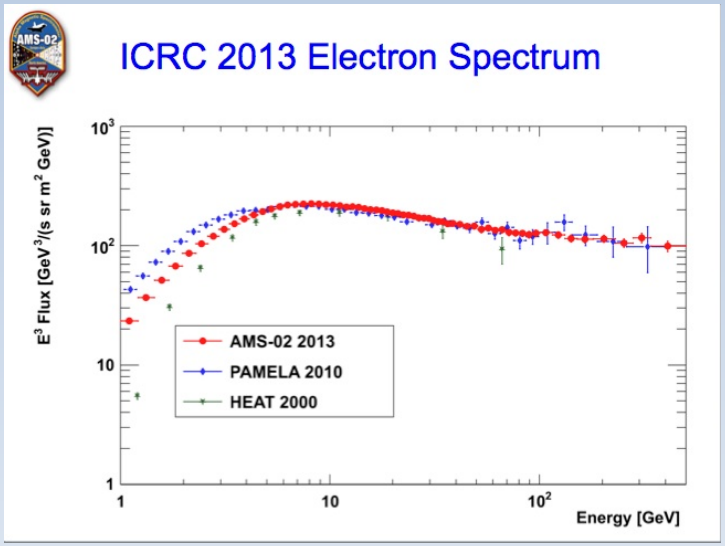
ICRC 2013 Electron Spectrum
E³ Flux [GeV³/(s sr m² GeV)]
Energy [GeV]
AMS-02 2013
PAMELA 2010
HEAT 2000

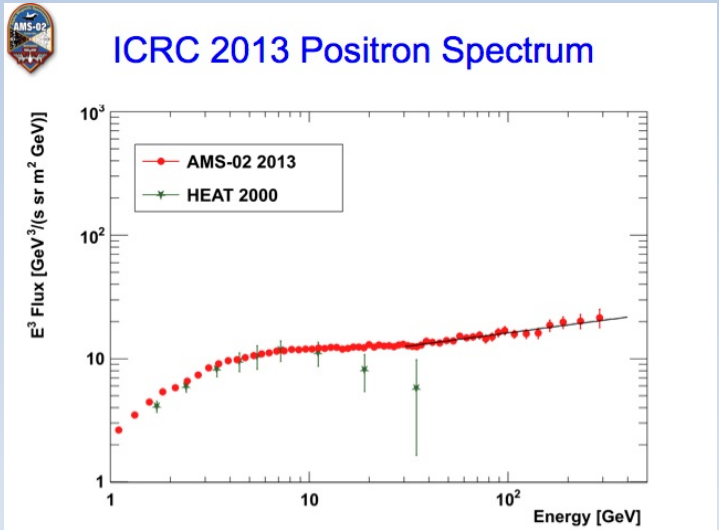
ICRC 2013 Positron Spectrum
E³ Flux [GeV³/(s sr m² GeV)]
Energy [GeV]
AMS-02 2013
HEAT 2000

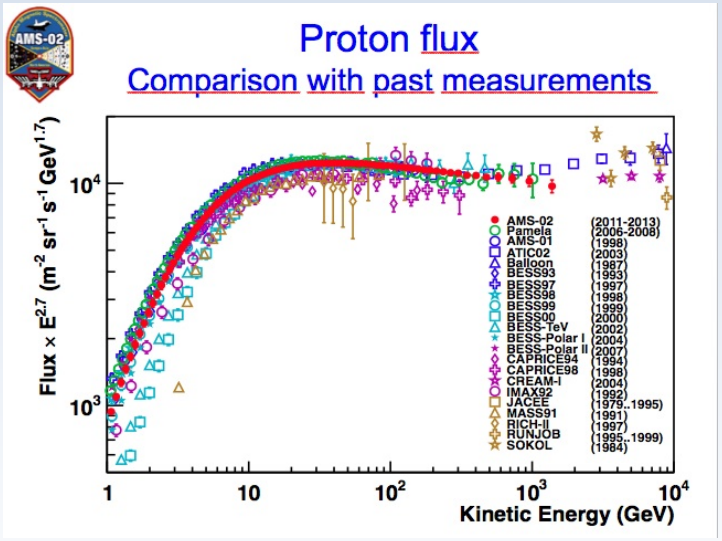
Proton flux
Comparison with past measurements
Flux × E^2.7 (m^-2 sr^-1 s^-1 GeV^1.7)
Kinetic Energy (GeV)
AMS-02 (2011-2013)
Pamela (2006-2008)
AMS-01 (1998)
ATIC02 (2003)
Balloon (1987)
BESS93 (1993)
BESS97 (1997)
BESS98 (1998)
BESS99 (1999)
BESS00 (2000)
BESS-TeV (2002)
BESS-Polar I (2004)
BESS-Polar II (2007)
CAPRICE94 (1994)
CAPRICE98 (1998)
CREAM-I (2004)
IMAX92 (1992)
JACEE (1979..1995)
MASS91 (1991)
RICH-II (1997)
RUNJOB (1995..1999)
SOKOL (1984)